AD-A063 530 GENERAL DYNAMICS CORP FORT WORTH TX FORT WORTH DIV F/G 17/8
F-16 ADVANCED ELECTRO-OPTICAL POD FIELD-OF-VIEW SIMULATION STUD--ETC(U)
DEC 78 F33657-78-C-0290
UNCLASSIFIED FZM-6817 NL

1 OF 2
AD
A063530

LEVEL II

FZM 6817
13 December 1978

(2)

AD A063530

F-16 ADVANCED ELECTRO-OPTICAL POD FIELD-OF-VIEW SIMULATION STUDY FINAL REPORT

CONTRACT NO. F33657-78-C-0290

DDC FILE COPY

This document has been approved for public release and sale; its distribution is unlimited.

DDC RECEIVED JAN 19 1979 C

This document contains Technical Data considered to be a resource under ASPR 1-329.1(b) and DoD Directive 5400.7 and is not a "record" required to be released under the Freedom of Information Act.

GENERAL DYNAMICS
Fort Worth Division
P.O. Box 748, Fort Worth, Texas 76101

78 12 26 067

(12) 123p.

(14) FZM-6817

(11) 13 December 1978

GENERAL DYNAMICS
Fort Worth Division

(6) F-16 ADVANCED ELECTRO-OPTICAL POD FIELD-OF-VIEW SIMULATION STUDY,

(9) FINAL REPORT.

CONTRACT NO. (15) F33657-78-C-0290

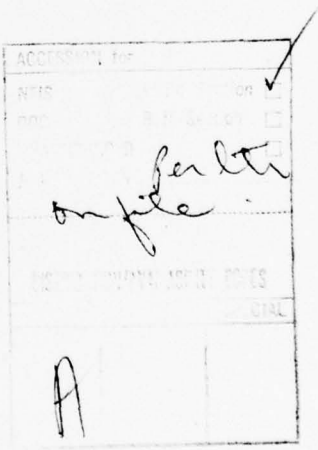

78 12 26 007
402 709

TABLE OF CONTENTS

LIST OF ILLUSTRATIONS

LIST OF ILLUSTRATIONS (continued)

LIST OF TABLES

LIST OF TABLES (continued)

SUMMARY

An F-16 advanced electro-optical (EO) pod field of view (FOV) simulation study was accomplished to determine the effects of sensor FOV and field-of-regard (FOR) on the pilot's workload and ability to locate, acquire, and attack targets in a day weapons-delivery environment. The simulated EO pod had a slewable TV sensor and laser designator head with two selectable FOVs for the TV sensor (wide and narrow FOVs), selectable area correlation and contrast tracking modes, and the capability to be either slaved to a preprogrammed set of coordinate or slaved to the aircraft's velocity vector. Three combinations of wide and narrow FOV pairs representative of current EO pod designs were examined - 6 and 1.5 degrees, 6 and 0.86 degrees, and 3 and 0.86 degrees. The three FOV pairs were evaluated subjectively and objectively in three experiments. Each experiment was designed around a laser-guided weapon and a corresponding weapon delivery mode. The weapons simulated in the study were chosen from current and potential (weapons under development) laser-guided ordnance -- GBU-10, Laser Guided Maverick, and Sabre. The weapon-delivery modes simulated were derived from basic F-16 avionics capabilities. The weapons and weapon delivery modes were chosen to interact with the FOVs of the simulated EO pod so that each FOV pair could be evaluated under separate acquisition range, weapons delivery, and target constraints.

For the three experiments, interdiction mission scenarios were designed around a high-threat, Central European environment that included simulated visibility and weather-ceiling restrictions. Pilots employed high-speed low-altitude egress to counter the simulated threat and weather environment.

In each experiment, the three FOV pairs were evaluated at long, intermediate, and short aircraft-to-target ranges. The ranges were based on typical visibility restrictions in the Central European region and on weapons-delivery constraints. The ranges were controlled through prebriefed pop-up points and the activation of the EO pod video at specific aircraft-to-target ranges. With three data run replications planned for each range point, each experiment contained a total of 27 data runs (3 FOV pairs X 3 ranges X 3 replications = 27 data runs).

Subjective data from each participating pilot were obtained through questionnaires. In the questionnaires, pilots rated each FOV pair by workload and system effectiveness at the completion of each experiment and at the completion of all experiments. Objective data were obtained from each data run through measures of specific parameters related to pilot workload and system effectiveness. Workload measures were total time to acquire (lock on) the target and the number of pod-related events to acquire (lock on) the target. Pod-related events consisted of pod-sensor slewing events, target designation events, and FOV changes. Effectiveness measures consisted of target acquisition and weapons delivery success rates. Other objective measures were target acquisition and weapons delivery ranges.

Six of eight pilots scheduled to participate in the study completed all the experiments. Two pilots did not complete the experiments because of a facility breakdown. The analysis of pilot ratings determined that the 6^{o} and 1.5^{o} FOV pair provided the least pilot workload and the most system effectiveness. Analysis of the objective workload measures determined that the 6^{o} and 1.5^{o} FOV pair provided the lowest pilot workload over the three experiments. Analysis of the objective effectiveness measures did not determine any significant difference between FOV pairs. This was most likely due to the small subject population and the large variance between pilot performance levels. The trends in the target acquisition and weapons release range indicated that the 6^{o} and 1.5^{o} FOV pair provided the longest target acquisition and weapons release ranges. Analysis of narrow-FOV utilization determined that narrow-FOV usage for target acquisition was significantly higher in the 1.5^{o} narrow FOV.

The pod-sensor FOR was evaluated through analysis of pod-seeker line-of-sight warning, obscuration, and gimbal limit data. A simulated pod-seeker line-of-sight obscuration limit was implemented in the simulator on the basis of actual F-16 aircraft/stores masking - with the pod mounted at the lower right side of the air inlet. For convenience of analysis, the pod-seeker gimbal limits were defined from 150 to 180 degrees of azimuth at zero degrees of elevation (see Figure 1.1-4, page 7). In addition, a warning tone was provided to the pilots that had an onset 10 degrees below the obscuration and gimbal limits. Analysis of the pod-seeker line-of-sight warning, obscuration, and gimbal limit data from the data runs determined that

1. Pilots responded well to the warning in that out of 255 warnings only 90 resulted in pod-seeker line-of-sight obscuration or gimbal limit.

2. The largest percentage of pod-seeker gimbal limits occurred between 160 and 170 degrees of azimuth.

From the results of the FOV and FOR analyses, it is concluded that

1. Given the mission and environment simulated and the simulator constraints, the 6^{o} and 1.5^{o} FOV pair provide the lowest pilot work-load and the best system effectiveness of the three FOV pairs evaluated.

2. Pod-sensor gimbal back-look limits between 160 and 170 degrees accommodated the majority of pod-sensor gimbal limits required for laser guided bomb delivery in the study.

3. Because of excellent pilot response to the pod line-of-sight obscuration and gimbal limit warning in the study, consideration should be given to the implementation of a warning system on aircraft carrying an advanced EO pod.

SECTION 1

INTRODUCTION

The F-16 advanced electro-optical (EO) pod field-of-view (FOV) study was accomplished by General Dynamics at Martin-Marietta's Simulation and Test Labcratory (STL) under contract to the United States Air Force, Aeronautical Systems Division (ASD). The study was conducted to aid ASD in defining pod field-of-view and field-of-regard requirements for a daylight advanced EO pod employed from an F-16 type fighter aircraft. The study was confined to the examination of three FOV pairs, provided by ASD/AER, which are representative of current EO pod designs. The three FOV pairs were evaluated in a simulated Central European weapons delivery environment by TAC pilots employing current and potential laser-guided weapons, weapons delivery modes derived from basic F-16 avionics capabilities, and up-to-date tactics. The objective of the study was to determine which FOV pair created the lowest pilot workload and the greatest effectiveness in locating, acquiring, and attacking targets in the simulated environment. In addition, pod-sensor gimbal angles were investigated during target attacks from weapon delivery to weapon impact to determine the pod field-of-regard required by a pilot to successfully deliver laser-guided ordnance.

Before the simulation tests were conducted, a test plan (Reference 1) was prepared and submitted to the Air Force for approval. Since this plan is lengthy, it is summarized in this report for convenience (Section 2) so that along with the information provided in the following sections (Sections 3, 4, and 5), a coherent final report would result. Also, details on the statistical equations used to achieve the study results, the supportive data from which the study results were derived, and a detailed description of the simulation facility are provided in three appendixes (Appendixes A, B, and C, respectively).

SECTION 2

SIMULATION DESCRIPTION

2.1 Simulation Configuration

2.1.1 Simulation Facility

The study was conducted at the Simulation and Test Laboratory (STL) of the Martin Marietta Corporation, Orlando, Florida. The simulation was mechanized through an F-16 cockpit mockup, analog and digital computers, a terrain board, and an electro-optical probe system. The F-16 cockpit mockup configuration was based on the full-scale development (FSD) aircraft and contained the controls and displays required to operate the aircraft and deliver various laser-guided weapons employing an electro-optical pod. The major controls and displays employed in the cockpit mockup are depicted in Figure 2.1-1.

The computer software implemented in the study consisted of an F-16 aerodynamic model adjusted for representative ordnance load; a model of the fly-by-wire flight control computer; a model of the integrated digital avionics system; and a model of the advanced EO pod, which included a SLAVE mode (pod sensor line-of-sight slaved to preselected coordinates or to the aircraft's velocity vector), an area correlation track mode, and a contrast track mode. Also implemented in the computers was the fire control logic, release constraints, ballistics, and heads-up display (HUD) symbology for each weapon system and delivery mode simulated.

The terrain board was 80-feet long by 40-feet wide which, at a scale of 1200 to 1, provided a 16 n.mi. by 8 n.mi. area of simulated terrain. Mirrors surround the terrain to provide the illusion of terrain extension. Motion excursion limits implemented in the computers to prevent the electro-optical probe system from damaging the mirrors limit the working area on the terrain board to an approximate 14 n.mi. by 7 n.mi area. The topography of the terrain board was characteristically Central European and contained all the natural and man-made features normally found in that region. A two-probe EO system was suspended over the terrain board by a gantry that was driven in combination with the terrain board to provide the flight simulation. The orientation of the two probes was fixed longitudinally. The North probe provided the video for the windscreen display at the cockpit mockup. The South probe, which was located 1 foot (1200 scale feet) behind and 2 inches (200 scale feet) below the North probe, provided the simulated EO pod video at the cockpit mockup.

An experimenter's console was also provided at the cockpit mockup. The console contained the necessary computer controls, video displays, and communication lines for the experimenter to

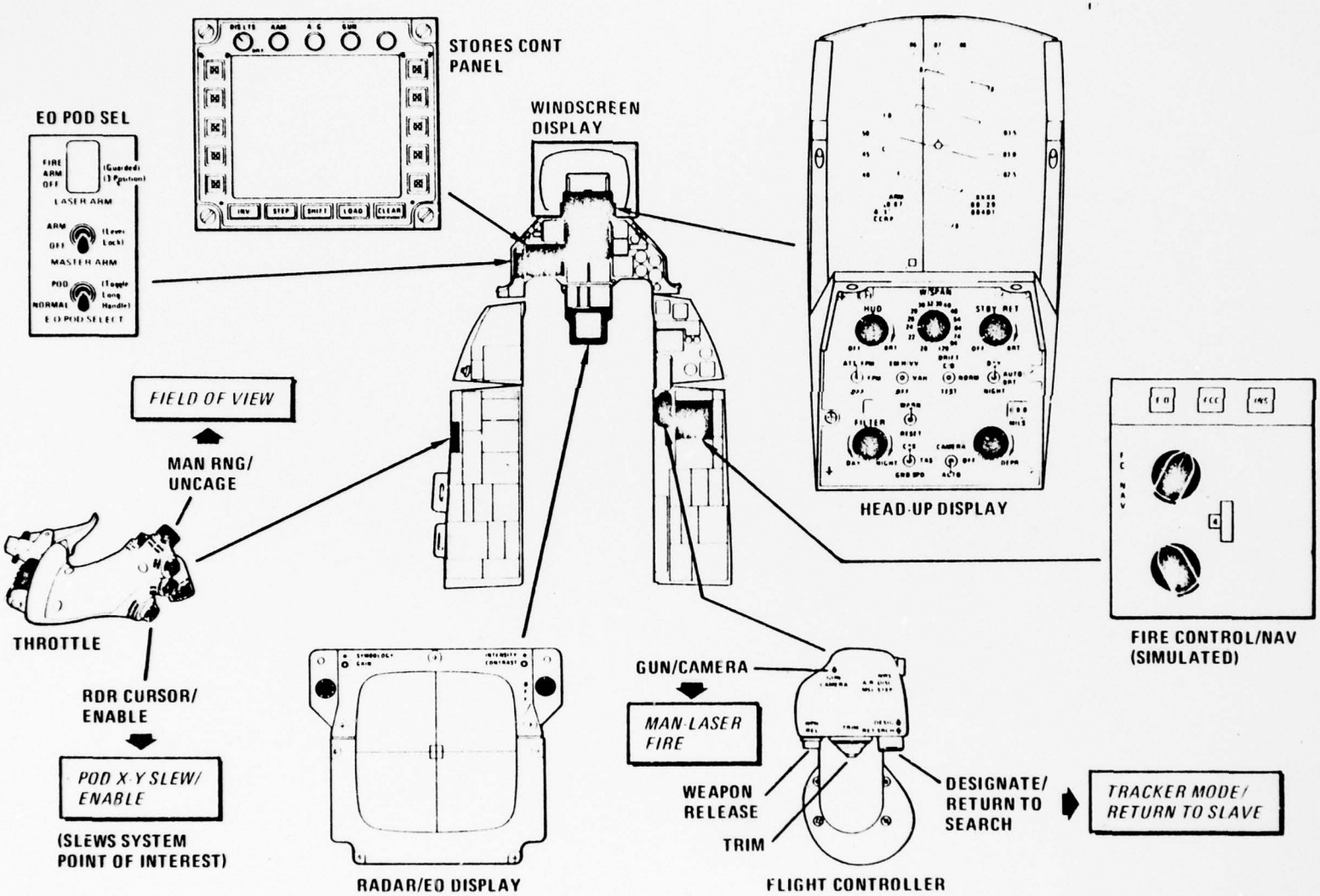

Figure 2.1-1 F-16 Cockpit Mockup Major Components

monitor and conduct all familiarization, training, and experimentation. Photographs of the simulation facility are provided in Figures 2.1-2 and 2.1-3. A detailed discussion of the simulation facility is contained in Appendix C.

2.1.2 Field-of-View Pairs

The following three field-of-view pairs were implemented in the study:

1. 6 degrees and 1.5 degrees
2. 6 degrees and 0.86 degree
3. 3 degrees and 0.86 degree

The original intent of the study was to evaluate a 1.5-degree and a 1-degree narrow FOV. Underscanning the 1.5-degree FOV to achieve a 1-degree FOV was attempted; however, the resultant video was unusable. Therefore, a new lens which provided an 0.86-degree FOV was manufactured by Martin Marietta. Although the video clarity provided by the 0.86-degree lens was degraded as compared with the 1.5-degree FOV, it was usable and was as close to the desired 1-degree FOV as was possible given the time and cost constraints of the study.

2.1.3 Field-of-Regard

For the purposes of the simulation, the assumed mounting location for the pod was on the lower right side of the F-16's air inlet (pod-seeker gimbal located at FS-178.24, WL-48, BL-20). At this location, the pod sensor masking limits were as described in Figure 2.1-4, assuming gimbal limits between 150 and 180 degrees of azimuth at zero degrees of elevation. Equations which approximated the true masking limits were developed and implemented in the computer, which yeilded the simulated aircraft/stores limits depicted in Figure 2.1-4. In addition, an aircraft/stores masking and gimbal limit warning which provided a warning tone to the pilot 10 degrees below the simulated limits was implemented in the simulator. The warning onset is also depicted in Figure 2.1-4.

2.1.4 Weapons and Weapons Delivery Modes

Weapon simulations implemented for the study consisted of a laser-guided bomb (LGB) with MK-84/GBU-10 ballistics and characteristics; a standoff- range laser-guided missile (LGM) with laser-

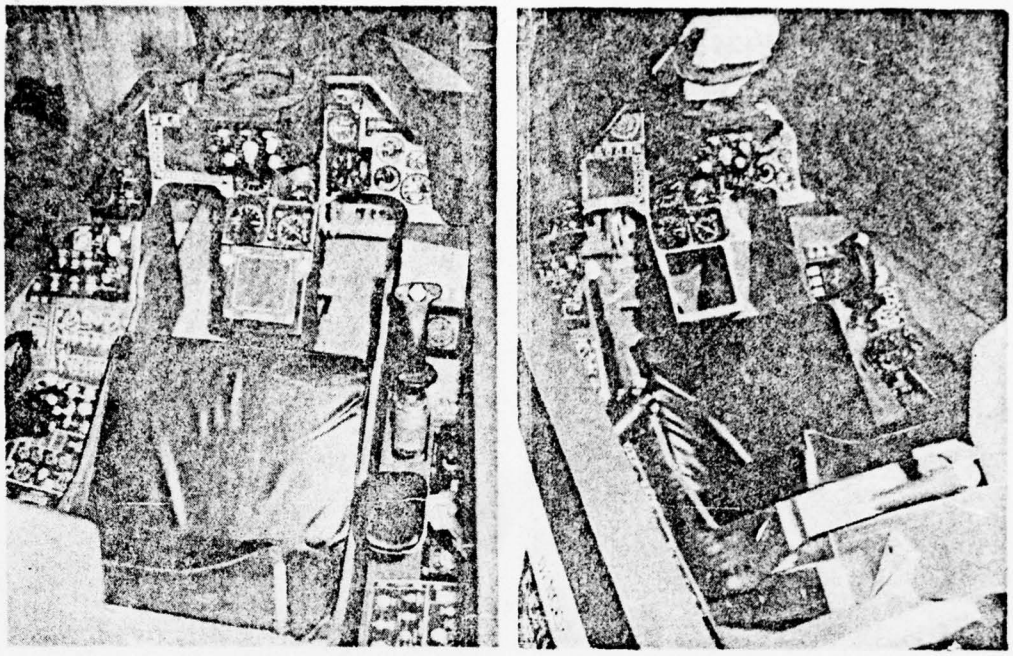

2 Views of F-16 Cockpit Mockup

Analog and Digital Computer Lab

Figure 2.1-2 Simulation Facility

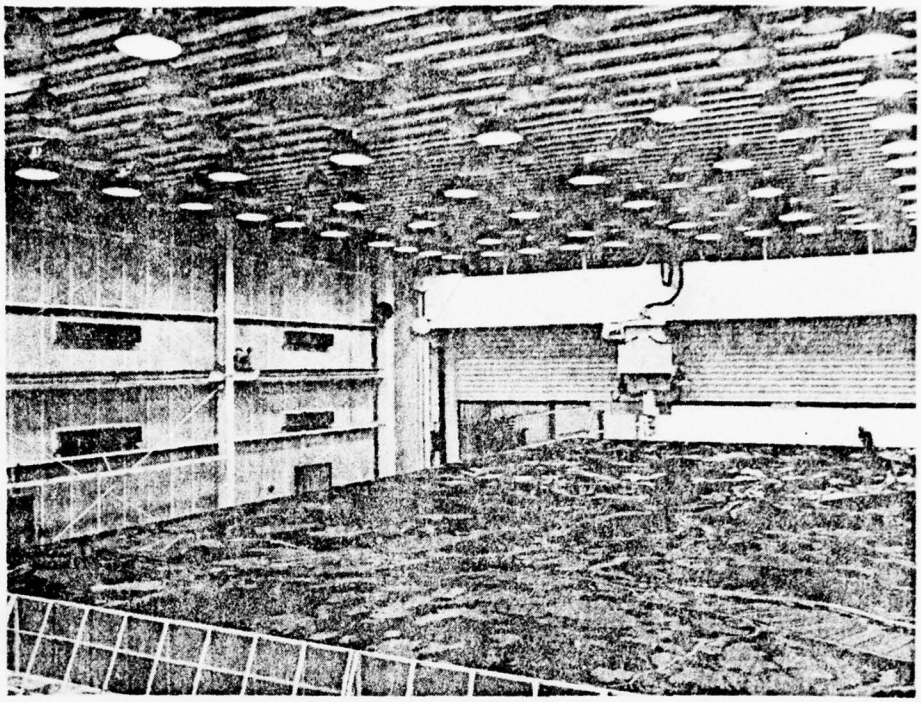

Terrain Board

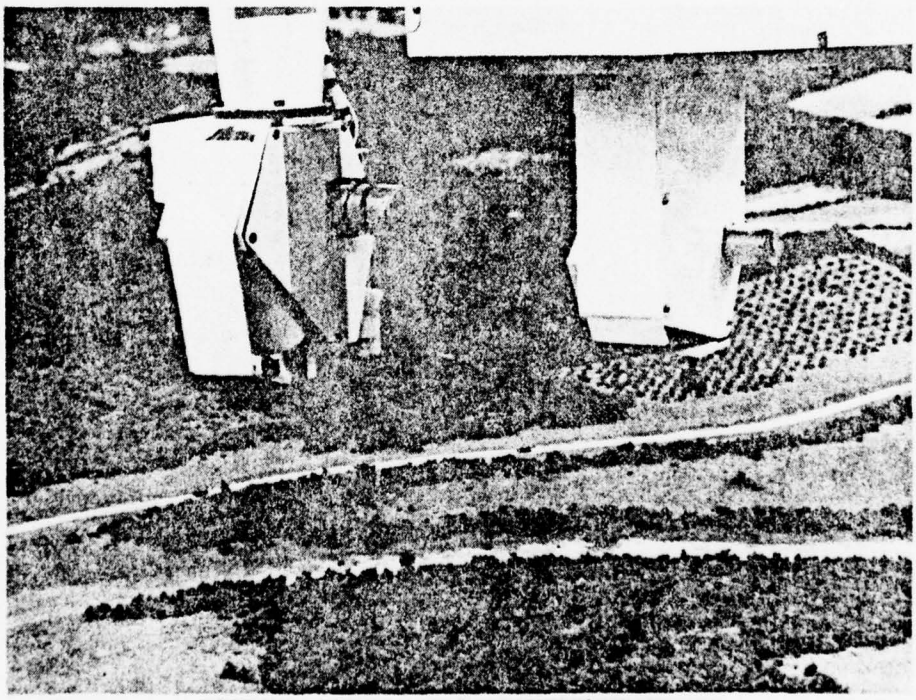

2-Probe Electro-Optical System

Figure 2.1-3 Simulation Facility

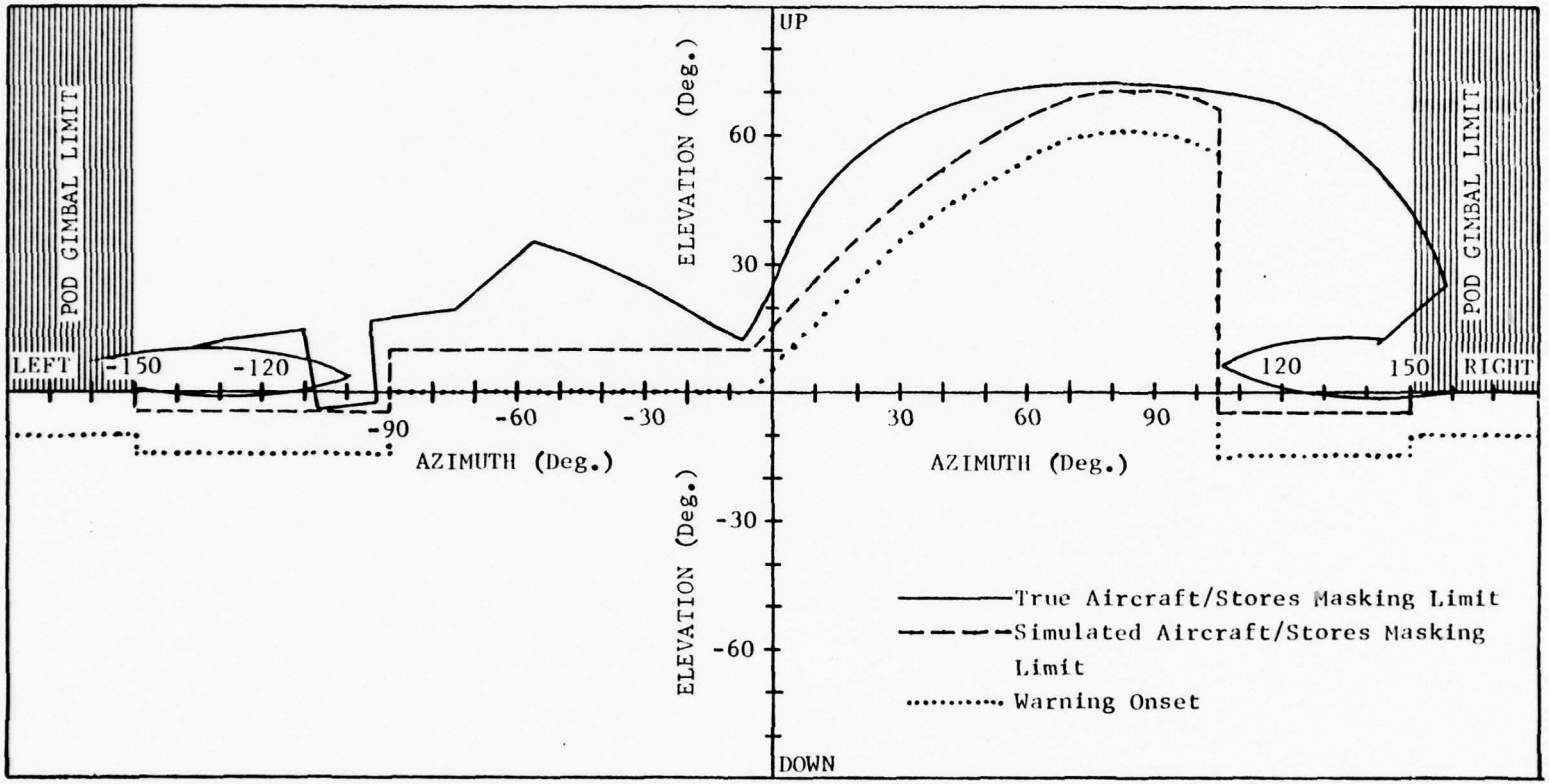

Figure 2.1-4 Pod Sensor Line-of-Sight Aircraft/Stores Masking, Gimbal Limits, and Warning Onset

guided Maverick characteristics; and a short-range, light-weight, laser-guided missile (LWLGM) with Sabre characteristics.

Weapons delivery modes for the study were created from basic F-16 avionics capabilities to support the weapon system and missions chosen for the study. The standard F-16 Continuously Computed Release Point (CCRP) weapons delivery mode was simulated for the delivery of laser-guided bombs against prebriefed targets. This mode provided head-up and head-down cueing and steering to a preprogrammed set of target coordinates and head-up weapons release solution cues for weapons delivery. Employing this mode, the pilot had the capability to toss, to deliver level, or to dive-deliver the weapon at the target.

A candidate laser-guided Maverick head-up delivery mode was simulated for attacking prebriefed targets. Missile acquisition and launch symbology was implemented on the head-up display for weapon delivery, and target cueing was provided on the head-up and head-down displays as in the CCRP weapons delivery mode.

A candidate visual target-acquisition weapon delivery mode for attacking targets of opportunity was simulated for the delivery of the light-weight laser-guided missile. In this mode the seeker head of the missile and line of sight of the EO pod were initially slaved to the flight path of the aircraft. Because this technique is found in the dive-toss weapons delivery modes on aircraft, this mode was named the Laser Guided Missile Dive Toss (LGMDT) weapons delivery mode. Missile acquisition and launch symbology was implemented on the head-up display as in the Maverick mode.

In addition to the weapons delivery modes, the F-16 navigation (NAV) mode was simulated to provide the pilot with the means to steer to a waypoint prior to target attack. The weapons, weapons delivery modes, and navigation mode simulated for this study are summarized in Figure 2.1-5.

2.1.5 EO Pod/Weapon/Weapon Delivery Mode Interaction

The weapons, weapon delivery modes, and attack scenario employed in the study were chosen to have a specific impact on the requirements for an EO pod. The LGB/CCRP combination was chosen to investigate the impact of aided target acquisition (target cueing) and weapons delivery from medium to short ranges on the pod sensor wide and narrow fields of view. Since the LGB has the longest time of flight, it was also chosen for its impact (following weapon release) on the pod sensor field-of-regard require-

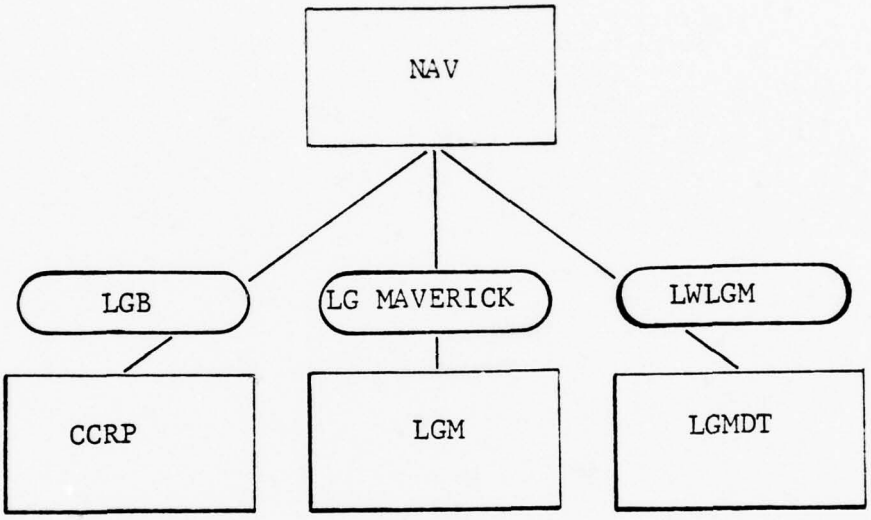

Figure 2.1-5 Simulated Weapons and Weapon Delivery Modes

ments. The LG Maverick/LGM combination was chosen to investigate the impact of aided target acquisition and weapon delivery from stand-off ranges on the EO pod sensor narrow fields of view. The LWLGM/LGMDT combination was chosen to investigate the impact of unaided (visual) target acquisition and weapons delivery from close ranges on the EO pod sensor wide fields of view. The EO pod/weapon/weapon delivery mode interactions are summarized in Table 2.1-1.

2.2 Experimental Method

The experimental design, the evaluation basis, and the data retrieval system employed in the study are described briefly below. Details are given in Reference 1, Sections 4 through 7, pages 20 through 58.

2.2.1 Scenarios for FOV Evaluation

Interdiction missions were simulated in the study. For laser guided bombs, a deep interdiction mission (40 miles behind the FEBA (Forward Edge of the Battle Area) against prebriefed fixed targets was simulated. Targets consisted of bridges, POL storage tanks, aircraft hangers, etc. For the laser-guided Maverick, two interdiction missions were simulated -- interdiction (1-5 miles behind the FEBA) against groups of armored vehicles in battle arrays, and interdiction (40 miles behind the FEBA) against both armored vehicles in battlefield and linear arrays and fixed hardened targets (aircraft revetments, bunkers, etc). For the LWLGM, an armed reconnaissance mission behind the FEBA against armor in both linear and battlefield arrays was simulated.

With the exception of the Maverick shallow interdiction mission, the mission profile was low-altitude (500 feet AGL), high-speed (540 KTAS) ingress, pop-up for target acquisition and weapons delivery, and low-altitude (500 feet AGL) egress. The ingress altitude was set at 500 feet in lieu of multiple altitudes of 250, 500, and 1000 feet owing to the need to limit the length of the tests because of simulator facility availability. The Maverick shallow interdiction mission was conducted at 2000 feet and 540 KTAS for ingress so that target acquisition could be examined at long range. The attack scenarios employed for each weapon and weapon delivery mode are depicted in Figures 2.2-1 through 2.2-4.

A Central European environment was simulated. The simulated environment included West German topography on the model board, limited visibility (3 to 6 n.mi), and a low weather ceiling (2500 feet MSL). Since actual visibility restrictions (smoke,

Table 2.1-1 EO POD/WEAPON/DELIVERY MODE INTERACTION

WPN/MODE	USEAGE CRITERIA	E-O POD IMPACT
LGB/CCRP	o CUEING TO TARGET o MEDIUM TO SHORT RANGE WEAPON DELIVERY (< 4.5 NM) o MEDIUM TO SHORT RANGE TARGET IDENTIFICATION & ACQUISITION (< 6 NM) o LONG WEAPON TIME-OF-FLIGHT	o WIDE & NARROW FIELDS-OF-VIEW o FIELD-OF-REGARD
LGMAV/LGM	o CUEING TO TARGET o LONG TO MEDIUM RANGE TARGET IDENTIFICATION & ACQUISITION (8 NM)	o NFOV ANALYSIS
LWLGM/LGMDT	o VISUAL ACQUISITION -- HUD o MULTIPLE, CLOSE-IN TARGET ENGAGEMENTS o SHORT WEAPON TIME-OF-FLIGHT	o WFOV ANALYSIS

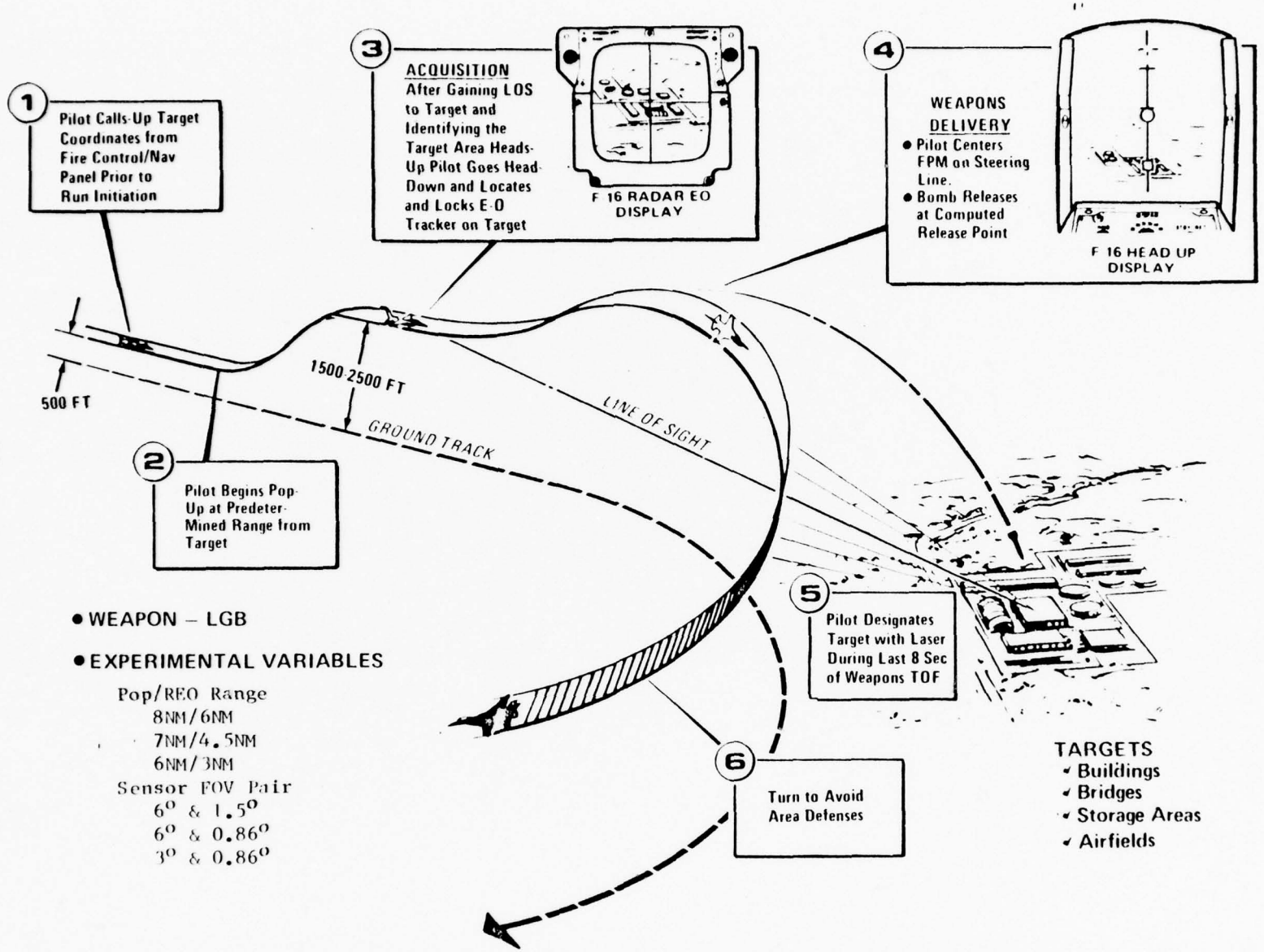

Figure 2.2-1 LGB/CCRP Target Attack Scenario

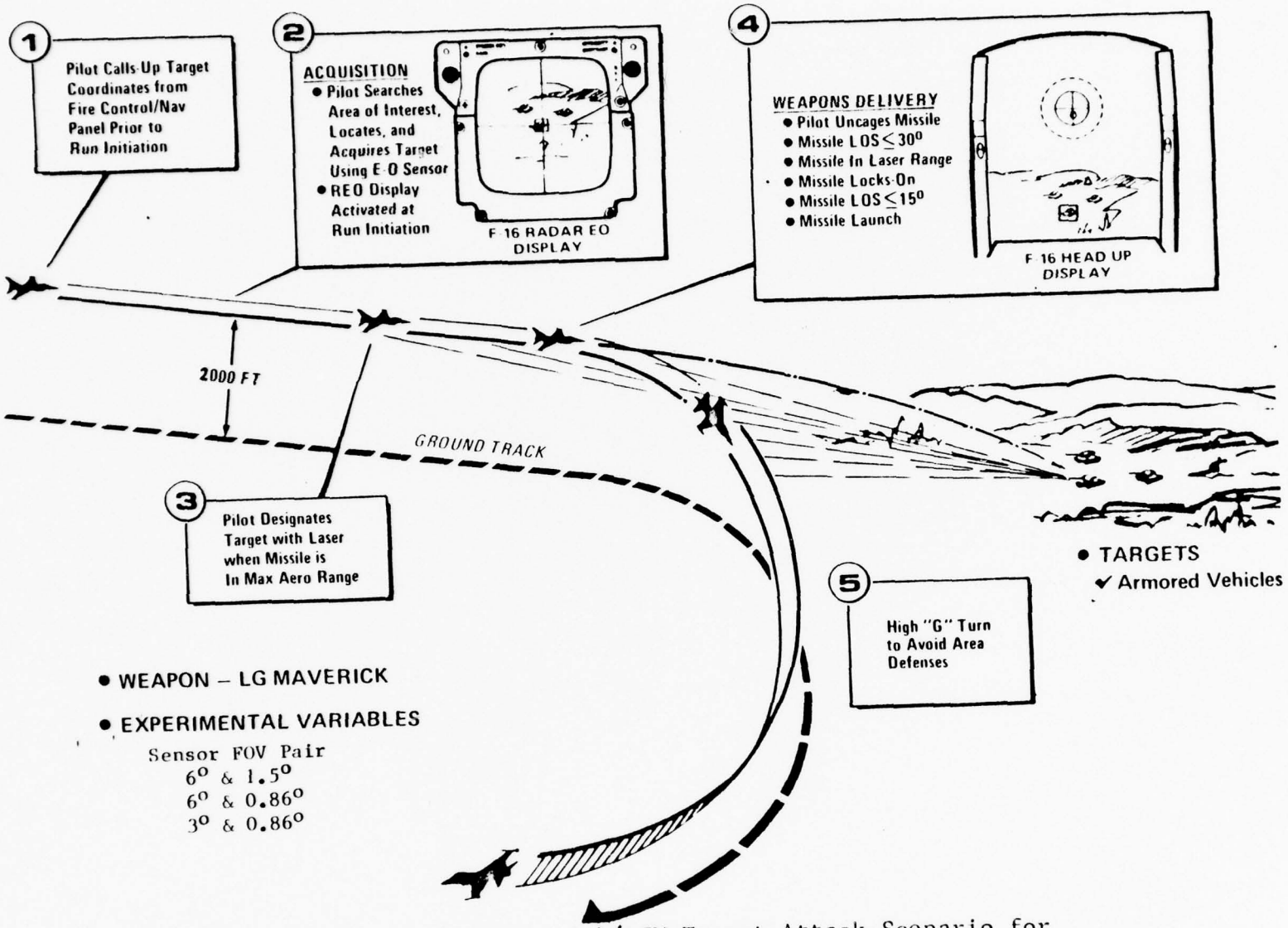

Figure 2.2-2 LG Maverick/LGM Target Attack Scenario for REO Display Activation at Run Initiation

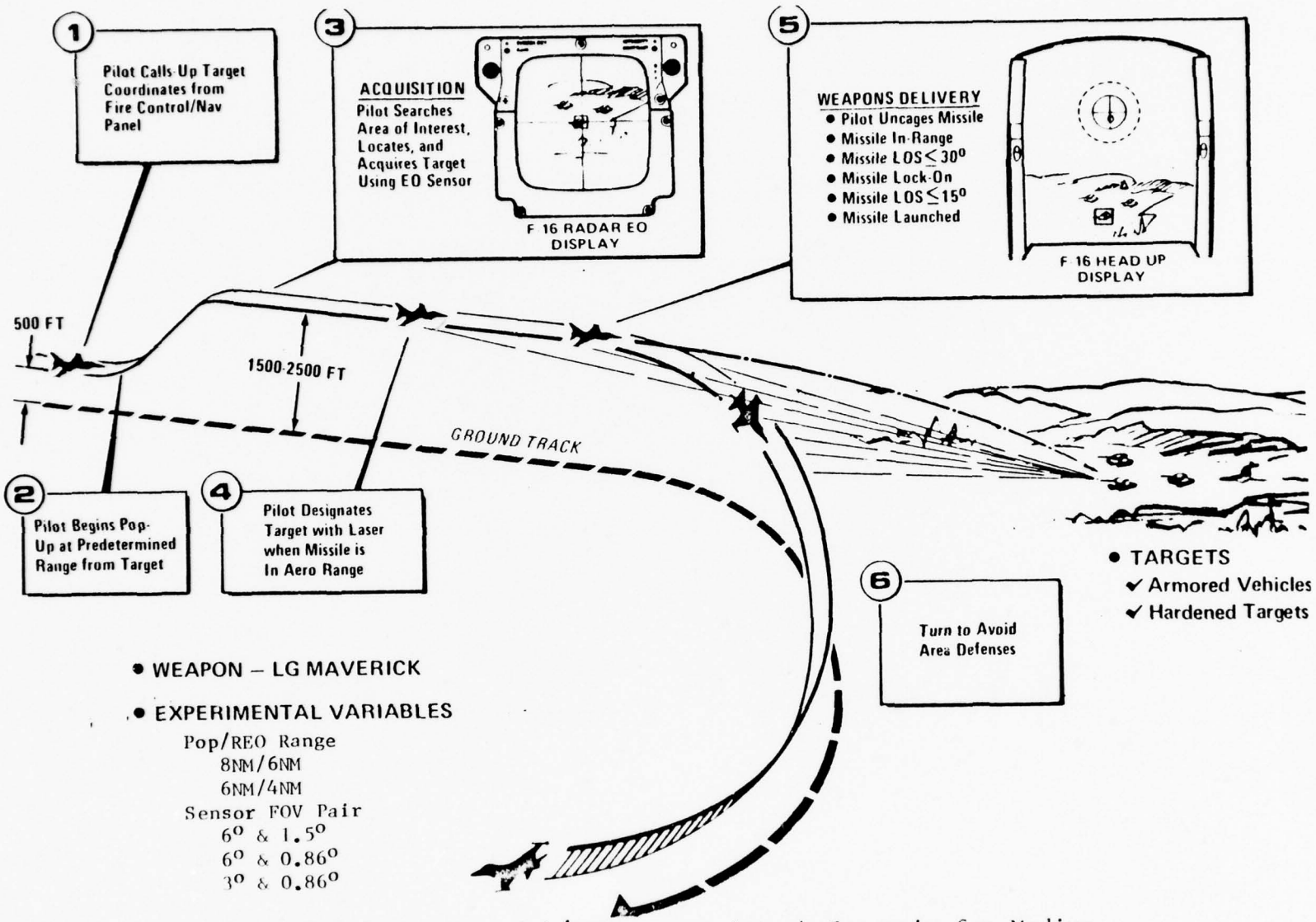

Figure 2.2-3 LG Maverick/LGM target Attack Scenario for Medium and Short REO Display Activation Ranges.

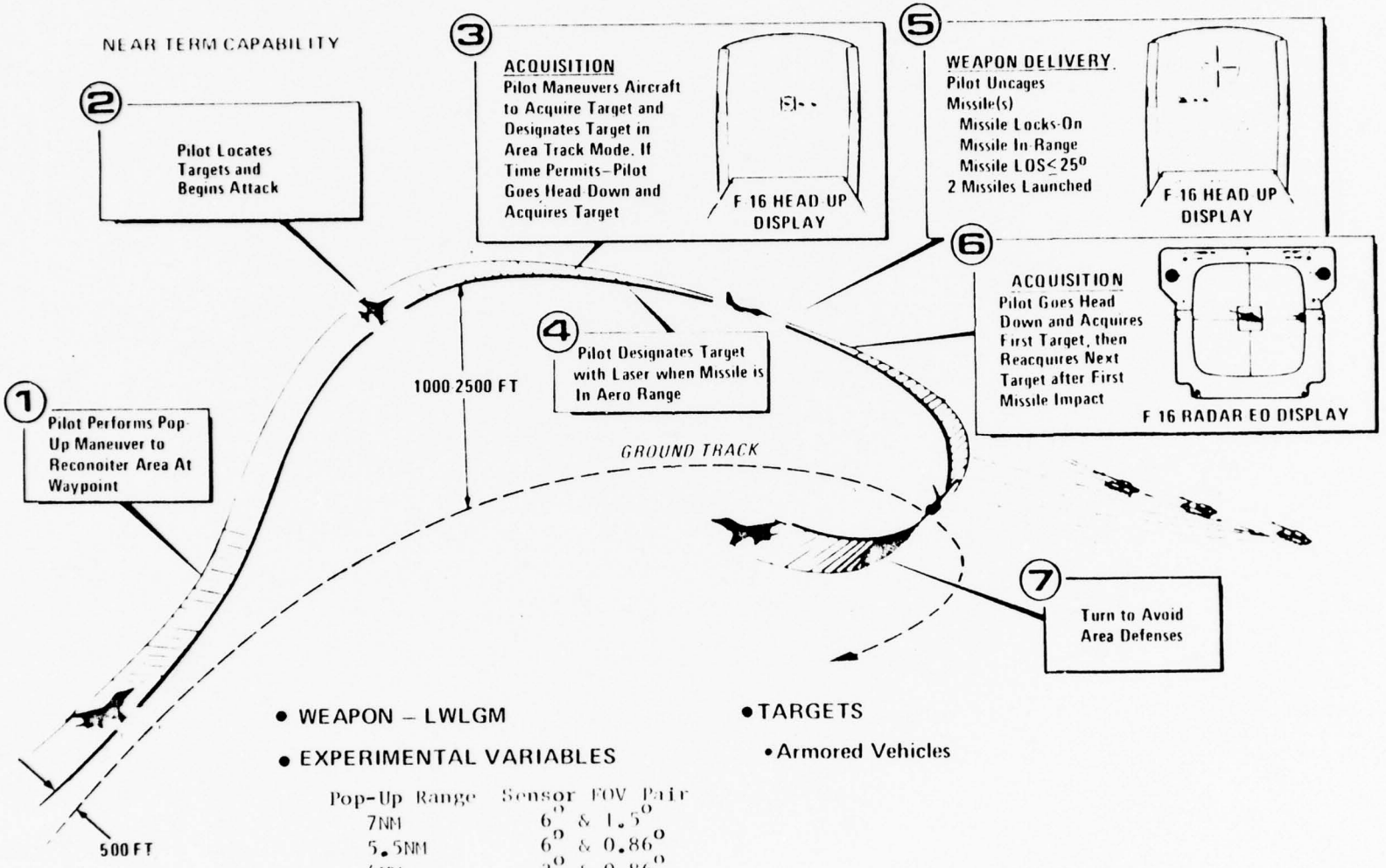

- WEAPON – LWLGM
- EXPERIMENTAL VARIABLES

Pop-Up Range	Sensor FOV Pair
7NM	6^{o} & 1.5^{o}
5.5NM	6^{o} & 0.86^{o}
4NM	3^{o} & 0.86^{o}

- TARGETS
  - Armored Vehicles

Figure 2.2-4 LWLGM/LGMDT Target Attack Scenario

haze, dust, etc.) could not be simulated, target visibility was denied to the pilot by using terrain masking during the low-altitude ingress and by turning the video off to the radar/electro-optical (REO) display until a specific range to target was reached. The weather ceiling was simulated by briefing the pilots to stay below 2500 feet MSL in their pop-up maneuvers and by penalizing them by scoring the run unsuccessful when they flew above the briefed altitude.

2.2.2 Experimental Design

The study consisted of three experiments. Each experiment was designed around a weapon and the corresponding weapon delivery mode -- LGB/CCRP, LG Maverick/LGM, and LWLGM/LGMDT--employing the attack scenarios described above. In each expierment, the pilot's ability to employ each of the FOV pairs at three pop-up/REO display activation ranges was investigated. The pop-up and REO display activation ranges were based on weapon capabilities and typical weather phenomena for the Central European environment. The detailed rationale for pop-up and REO display activation ranges in each experiment is given in Table 2.2-1. Three replications were planned for each FOV pair and pop-up/REO activation range combination. The resultant experimental matrix for each experiment had 27 data runs (3 FOV pairs X 3 pop-up/REO activation ranges X 3 replications = 27 data runs). The total of three experiments thus contained 81 data runs (3 experiments X 27 data runs/experiment).

So that the results of the simulation would not be influenced by unrealistic inertial target accuracy or by pilot memorization of target locations, additional parameters were varied. An error of 1000 feet was introduced with random azimuth for each pre-cued target to simulate inertial error and coordinate uncertainty. This error assumed an inertial update within 5 minutes of the target with an inertial drift rate of 1 n.mi/hr. Twelve targets were assigned to each of the three experiments (36 separate targets). To keep target study to an acceptable level, four separate targets were assigned to the nine data runs for each FOV pair. During the nine data runs for each FOV pair in an experiment, the four targets were ordered such that that pilot would not attack the same target without first attacking two other targets. No target was attacked more than three times. When the same target was attacked more than once, the run-in heading was varied at least 30 degrees so that the pilot never achieved the identical target aspect.

In each of the three experiments, nine sets of conditions were tested, each representing a unique combination of FOV pair and pop-up/REO activation range. Each set of conditions was repeated three times against different targets. The effects of tar-

TABLE 2.2-1 THREAT/WEATHER SIMULATION

WPN/DEL MODE	REO ACTIVATION RANGE (N.MI.) (WEATHER EFFECTS)	POP-UP RANGE (N.MI.) (THREAT & WEATHER EFFECTS)
LGB/CCRP (500' RUN-IN)	6 = MAX WPN RNG + 10 SECS 4.5 = INTERMEDIATE RANGE 3 ≈ TYPICAL DAY IN EUROPE	8 = REO ACT. + 2NM POP-UP TIME 7 = REO ACT. + 2NM POP-UP TIME + 3 SEC ORIENTATION TIME 6 = REO ACT. + 2NM POP-UP TIME + 6 SEC ORIENTATION TIME
LGM/LGM (500' RUN-IN) (2000' RUN-IN)	6 = APPROX. MAX WPM RNG 4 ≈ TYPICAL DAY IN EUROPE REO ON AT RUN INITIATION TO EVALUATE TARGET ACQUISITION FOR STAND-OFF WEAPON	8 = REO ACT + 2NM POP-UP TIME 6 = REO ACT + 2NM POP-UP TIME
LWLGM/LGMDT	REO ON AT RUN INITIATIONS NO VISIBILITY LIMITATION ASSUMED FOR ARMED RECCE MISSION	7 = MAX WPN RANGE + 2NM POP-UP TIME + 3 SEC ORIENTATION TIME + 10 SEC ACQ TIME 5.5 = INTERMEDIATE RANGE 4 = .5NM MIN RANGE + 10 SEC ACQ TIME (2.5NM) + 2NM POP-UP

get order and difficulty on the data were removed by systematically counterbalancing the nine conditions over the run matrices for three sets of two pilots. Therefore, six pilots had to complete all 81 of the data runs to fully counterbalance the data. The counterblanaced run matrices for each experiment are shown in Tables 2.2-2 through 2.2-4.

2.2.3 Subject Pilots

A total of eight subject pilots were requested from the United States Air Force Tactical Air Command to participate in the study. The request covered four A-7 qualified pilots from operational squadrons and four F-4 qualified pilots, two from an operational squadron at Eglin AFB, Florida, and two from Nellis AFB, Nevada. Pilots were to be randomly selected with the exception that none were to have experience flying the F-16 aircraft. The mix of A-7 and F-4 pilots was requested to obtain pilots with and without head-up-display (HUD) experience. The eight subject pilots are listed in Table 2.2-5 along with their experience.

2.2.4 Evaluation Basis

The evaluation of the FOV pairs was based on two data sources -- subjective data elicited from the pilots through questionnaries and objective data taken from parameter readouts provided by the simulation computer after each of the data runs. Because of the brevity of the experiments (small subject population and small number of replications for each data point), the primary data source was the subjective data.

For the FOV pair evaluation, both data sources were broken into two categories - pilot workload and system effectiveness. For the subjective analysis, pilots rated workload and system effectiveness for each FOV pair in each weapon delivery mode. The collective ratings were analyzed to determining which FOV pair provided the least workload and the most effectiveness over the three weapon delivery modes. For the objective analysis, separate measures were employed to determine pilot workload and system effectiveness. Pilot workload was evaluated by two measures. The first was to determine the time required by the pilot to locate, acquire (lock-on) and identify the target employing each FOV pair. Included in this measure was total time to locate acquire and identify the target in both wide and narrow FOVs and the time spent in each wide and narrow FOV. Since the pilot had to physically operate discrete switches and controls to search for, acquire and verify the target, the second workload measure was to sum the number of discrete switch and control operations related to the pod during this phase of the mission. These opera-

Table 2.2-2 COUNTERBALANCED LGB/CCRP RUN MATRICES

Note: Number inside matrices indicate sequence in which data runs were accomplished.

WEEK #1 PILOTS 1 & 2

REO RANGE / REPLICATIONS / FOV	6NM			3NM			4.5NM		
	1	2	3	1	2	3	1	2	3
6° & 1.5°	1	2	3	4	5	6	7	8	9
6° & 0.86°	10	11	12	13	14	15	16	17	18
3° & 0.86°	19	20	21	22	23	24	25	26	27

WEEK #2 PILOTS 3 & 4

REO RANGE / REPLICATIONS / FOV	3NM			4.5NM			6NM		
	1	2	3	1	2	3	1	2	3
6° & 0.86°	1				5				9
3° & 0.86°	10				14				18
6° & 1.5°	19				23				27

WEEK #3 PILOTS 5 & 6

REO RANGE / REPLICATIONS / FOV	4.5NM			6NM			3NM		
	1	2	3	1	2	3	1	2	3
3° & 0.86°	1				5				9
6° & 1.5°	10				14				18
6° & 0.86°	19				23				27

Table 2.2-3 COUNTERBALANCED LG MAVERICK/LGM MATRICES

Note: Numbers inside matrices indicate sequence in which data runs were accomplished.

WEEK #1 PILOTS 1 & 2

REO RANGE / REPLICATIONS / FOV	6NM			4NM			ARI		
	1	2	3	1	2	3	1	2	3
6° & 0.86°	1	2	3	4	5	6	7	8	9
6° & 1.5°	10	11	12	13	14	15	16	17	18
3° & 0.86°	19	20	21	22	23	24	25	26	27

WEEK #2 PILOTS 3 & 4

REO RANGE / REPLICATIONS / FOV	4NM			ARI			6NM		
	1	2	3	1	2	3	1	2	3
6° & 1.5°	1				5				9
3° & 0.86°	10				14				18
6° & 0.86°	19				23				27

WEEK #3 PILOTS 5 & 6

REO RANGE / REPLICATIONS / FOV	ARI			4NM			6NM		
	1	2	3	1	2	3	1	2	3
3° & 0.86°	1				5				9
6° & 0.86°	10				14				18
6° & 1.5°	19				23				27

Table 2.2-4 COUNTERBALANCED LWLGM/LGMDT RUN MATRICES

Note: Numbers inside matrices indicate sequence in which data runs were accomplished.

WEEK #1 PILOTS 1 & 2

POP-UP RANGE / REPLICATIONS / FOV	7NM			5.5NM			4NM		
	1	2	3	1	2	3	1	2	3
3° & 0.86°	1	2	3	4	5	6	7	8	9
6° & 0.86°	10	11	12	13	14	15	16	17	18
6° & 1.5°	19	20	21	22	23	24	25	26	27

WEEK #2 PILOTS 3 & 4

POP-UP RANGE / REPLICATIONS / FOV	5.5NM			4NM			7NM		
	1	2	3	1	2	3	1	2	3
6° & 1.5°	1				5				9
6° & 1.5°	10				14				18
3° & 0.86°	19				23				27

WEEK #3 PILOTS 5 & 6

POP-UP RANGE / REPLICATIONS / FOV	4NM			7NM			5.5NM		
	1	2	3	1	2	3	1	2	3
6° & 1.5°	1				5				9
3° & 0.86°	10				14				18
6° & 0.86°	19				23				27

Table 2.2-5 SUBJECT PILOTS

NAME/RANK	SQUADRON/BASE	AIRCRAFT/TOTAL TIME	EO EXPERIENCE
Anderson, Jim/Capt	59TFS/Eglin AFB Fl	F-4/2000 Hrs	PAVE SPIKE
Burroughs,Richard/Capt	75TFS/England AFB La	A-7/2650 Hrs	MAVERICK
Carter, Ted/Capt	354 TFS/Davis Monthan AFB Az	A-7/1230 Hrs	MAVERICK
Craig, John/Capt	414 FWS/Nellis AFB Nv	F-4/1400 Hrs	PAVE SPIKE
Moreau, Edward/Capt	4485 Test Sq/Eglin AFB Fl	F-4/1900 Hrs	MAVERICK,LATAR, PAVE SPIKE
Van Valkenburg, Fred/ 1/Lt	75 TFS/England AFB La	A-7/500 Hrs	MAVERICK
Wilder, David/Capt	TFWC/Nellis AFB Nv	A-7/1700 Hrs	None
Wilson, Gary/Capt	76 TFS/England AFB La	A-7/1275 Hrs	MAVERICK

tions included pod sensor slewing, target designation events, and pod FOV changes.

System effectiveness with each FOV pair was evaluated by two measures -- target acquisition success rates and weapons delivery success rates. Target acquisition success rates were used to measure system effectiveness during initial target search, acquisition and verification. Weapons delivery success rates were used to measure system effectiveness after initial target acquisition during weapons delivery and the designation turn. Target acquisition success was based on whether or not the pilot found the correct target and locked the pod on it outside the minimum weapons delivery range. The determination of weapons delivery success or failure was much more complex. The conditions for success were based on:

1. Meeting weapon release constraints

2. Tracking the target consistently (laser aiming) during the weapon's time-of-flight

3. Keeping the laser "ON" consistently during the weapon's time-of-flight.

Pod sensor field-of-regard requirements were evaluated through an analysis of pod line-of-sight warning and obscuration data. These data were applied to the aircraft masking and pod gimbal limits employed in the study to define the field of regard required by pilots to deliver laser-guided weapons from the F-16 aircraft.

2.3 Data Categories Evaluated

A brief description of the subjective and objective data evaluated in the study is given below. A complete description of the data collected during the course of the experiments is given in Reference 1, Section 7 and Appendix B.

2.3.1 Subjective Data

Three subjective data categories were evaluated in the study: pilot comments and observations, pilot FOV pair workload ratings, and pilot FOV pair effectiveness ratings. All subjective data were collected on debriefing forms employed after each data run, after each simulation period, after the completion of each experiment, and after the completion of all experiments.

Pilot comments and observations were summarized both from their direct responses to questions in the debriefing materials and from their unsolicited remarks regarding the pod FOV pairs. Following the completion of each experiment and after all experiments were completed, the pilots rated the relative workload and effectiveness associated with each FOV pair on a scale ranging from 0.0 to 10.0 for a series of four tasks:

1. Search for targets
2. Verify targets
3. Fly designation turn and maintain tracker on target
4. Perform complete mission (summary of all tasks).

Included in the ratings was one non-pod-related task, weapon delivery. An example of the questionnaire, showing the rating scale, is presented in Figure 2.3-1. Data were retrieved from the scales, which were exactly 10 cm long, by measuring the distance from the left-hand index to the point at which the pilot had indicated his rating for each FOV pair.

2.3.2 Objective Data

The objective data were subdivided into the following four categories:

1. Workload data
2. Effectiveness data
3. Other data (data collected to evaluate the FOV pairs which did not fit either workload or effectiveness categories)
4. Field-of-regard data.

The majority of the objective data was taken from parameters measured by the computer during each data run and printed immediately after the run. A sample end-of-run computer printout with pertinent events highlighted is shown in Figure 2.3-2.

2.3.2.1 Workload Data

As previously discussed, the workload data consisted of target acquisition time lines and pod-related events. In both the

Figure 2.3-1 Debriefing Questionnaire Example
(not to scale)

On those questions requiring a subjective rating, place an X and the field of view pair ($6^{\circ}/1\frac{1}{2}^{\circ}$, $6^{\circ}/1^{\circ}$, $3^{\circ}/1^{\circ}$) at the appropriate spot along the rating line.

Example:

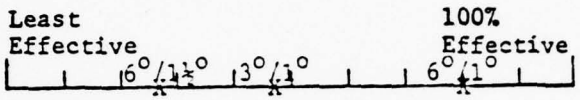

FOV Effectiveness

1. Rate the performance effectiveness of each FOV pair for each of the following tasks.

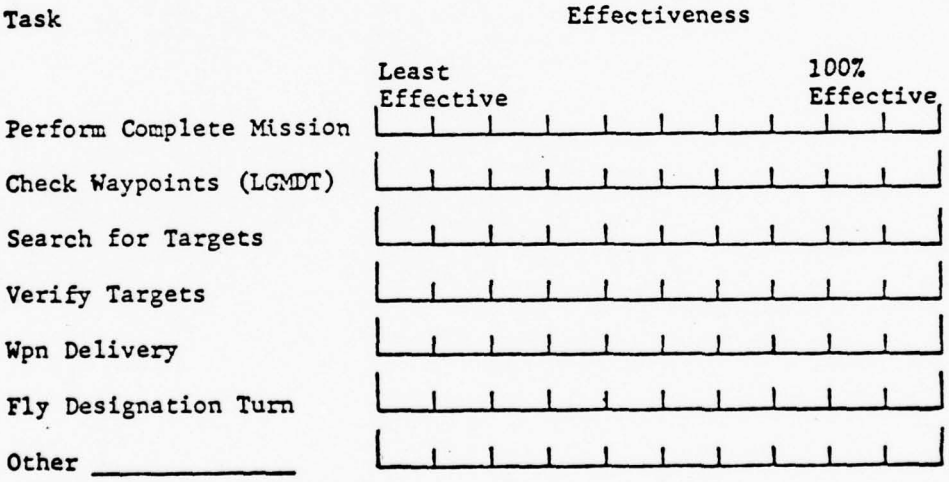

RUN NO. - 130
TIME, DATE - 2114 SEP 16,'78
PILOT'S NAME - WILDER
TARGET NUMBER - 5
ERROR VECTOR VALUES (X,Y,Z) 25. 750. 0.
WEAPON ID - BOMB
DELIVERY MODE - CCRP
POD FOVS- 6.M,.857
TEST ALTITUDE - 2000
TEST AIRSPEED - 540
REQ ACT RANGE - 3.0

EVENTS	ESTIM BLVPPA VAATTR VC EK	TIME SEC	SLANT RANGE FEET	MSL ALT FEET	RADAR ALT FEET	POD EL DEG	POD AZ DEG	ROLL DEG	PITCH DEG	HEADING DEG	ALT ERR FEET	VEL ERR KTS	STEER ERR DEG	FLT/FAIL TIME SEC	TAS KTS
FLIGHT BEGINS	110000	.0	42553	726	561	-2.1	-.1	-.0	1.3	53.0	-1273	0	-.1	.0	540
SLEW ENABLE	110000	20.7	24814	2308	2243	-6.0	1.6	2.2	.9	52.0	308	-28	.5	.0	519
SLEW DISABLE	110000	22.1	22645	2283	2236	-5.9	1.5	3.7	.5	52.1	283	-26	.4	.0	514
SLEW ENABLE	110000	24.5	20648	2257	2229	-6.5	1.0	4.9	.4	52.8	257	-23	.9	.0	517
SLEW DISABLE	110000	25.0	19933	2249	2222	-5.8	.8	3.4	-.4	52.8	249	-23	.2	.0	517
SLEW ENABLE	110000	25.2	19787	2242	2214	-5.8	.7	3.3	-.4	52.8	242	-22	.2	.0	518
SLEW DISABLE	110000	25.6	19382	2230	2210	-5.8	.6	3.2	-.4	52.8	230	-22	.1	.0	518
SLEW ENABLE	110000	25.9	19066	2218	2195	-5.8	.5	3.2	-.5	52.9	218	-21	.1	.0	519
SLEW DISABLE	110000	26.2	18819	2200	2185	-5.8	.5	3.2	-.5	52.9	200	-21	.1	.0	519
REQ ACT RANGE	110000	26.9	18183	2174	2176	-6.0	.5	3.1	-.5	53.0	174	-19	.1	.0	521
SLEW ENABLE	110000	29.2	16142	2139	2104	-2.8	.1	1.3	2.6	53.2	139	-17	-.0	.0	523
*DESIGNATE	110000	30.3	15342	2159	2064	-10.5	-.3	1.2	2.9	53.2	159	-17	-.1	.0	523
SLEW DISABLE	100010	30.4	15270	2159	2044	-10.3	-.2	1.2	2.9	53.2	159	-17	-.1	.0	523
AREA TRACK	101000	30.5	15848	2164	2029	-10.3	-.2	1.2	2.9	53.3	164	-17	-.1	.0	523
MARK	101001	31.0	15669	2169	1931	-10.5	-.4	1.2	2.9	53.3	169	-16	-.2	.0	524
BOMB PICKLE	101000	32.9	13553	2218	1958	-11.3	-.9	-1.5	2.5	53.3	218	-16	-.2	.0	524
COMPUTED RELEASE	101000	34.4	12455	2259	2082	-18.7	-1.6	-5.3	9.3	52.3	259	-17	-.0	.0	523
										MAXIMUM STEERING ERROR -			6.1		
WEAPON RELEASE	101000	34.5	12419	2264	2084	-19.4	-1.4	-5.3	9.8	52.2	264	-17	-.0	14.5	523
*LASER TRIGGER	101000	36.8	10399	2662	2422	-4.4	-28.7	-93.9	14.3	48.3	662	-27	-.0	12.1	513
SLEW ENABLE	100010	39.1	8584	3048	2885	-24.4	-30.8	-91.9	7.4	26.8	1048	-37	-.0	9.8	503
MARK	100011	40.1	7995	3138	2971	-37.2	-33.0	-88.5	5.7	16.4	1138	-42	-.0	8.8	498
SLEW DISABLE	101000	40.8	7798	3184	2992	-45.9	-35.6	-86.7	4.8	9.5	1184	-45	-.0	8.2	495
AREA TRACK															
*LASER IGNITION	101000	40.9	7830	3189	2989	-47.4	-36.1	-84.7	4.7	8.5	1189	-46	-.0	8.1	494
MARK	101001	41.0	7773	3201	2997	-49.0	-38.4	-88.0	4.3	6.8	1201	-46	-.0	7.9	494
POD LOS WARNING	101000	46.7	8388	3338	3148	-8.6	-153.6	-99.6	-2.4	287.7	1338	-84	-.0	2.2	454
OBSCURED LOS	101000	47.3	8927	3326	3148	.9	-153.6	-97.2	-6.4	278.4	1326	-87	-.0	1.6	453
UNOBSCURED LOS	101000	47.7	9119	3292	3114	-2.0	-155.4	-72.0	-3.1	274.5	1292	-89	-.0	1.2	451
POD LOS WARNING															
WEAPON IMPACT	101000	49.0	10080	3216	3029	-13.6	-149.8	-36.5	1.1	275.4	1216	-88	-.0	.0	452
POD LOS WARNING	101001	49.3	10345	3214	3024	-9.2	-147.2	-43.1	2.0	273.3	1214	-87	-.0	.0	453
MARK															

Figure 2.3-2 End-of-Run Data Listing Example

LGB/CCRP and LG Maverick/LGM experiments, the time to search, acquire (lock-on) and verify the target was determined in each run by measuring the time from REO activation to target acquisition. Acquisition of the target was determined by the experimenter, who placed a "MARK" in the data when the pilot designated (locked the pod tracked on) the correct target. The pod-related events performed to search, acquire (lock-on), and verify the target were summed from REO activation to target acquisition.

In the LWLGM/LGMDT experiment, the REO display was on throughout the run; therefore, a different technique for measuring acquisition time and pod-related events was applied. Following the pop-up maneuver, pilots did not go head-down and begin slewing the pod sensor to search for the target until they located the suspected target area heads-up on the windscreen display. Therefore, the time to search, verify, and acquire the target employing the EO pod was measured from the first slewing event following the pop-up maneuver to target acquisition. Pod-related events were measured by the same criteria.

2.3.2.2 Effectiveness Data

Effectiveness data consisted of acquisition and weapons delivery success/failure data for each run accomplished over the three experiments. Acquisition success was initially determined at the experimenter's console, where he placed a "MARK" in the data when the pilot successfully acquired (locked-on) the correct target with the EO pod. The acquisition success was later confirmed by reviewing the data printout to determine if the acquisition was made outside minimum weapons delivery constraints. In a few instances, either the experimenter forgot to insert the mark in the run event data or the computer malfunctioned and did not produce a good end-of-run printout. In these instances, the video tape made during the run was reviewed to ascertain the acquisition success/failure.

Weapons delivery success was determined after examination of the data from the individual runs. During a run, the experimenter would watch for specific events and conditions to occur. These included successful target acquisition, weapons release, consistency of target tracking, consistency of laser designation, and obscuration warning cues. When a run appeared to be successful on the basis of observation, a mark was entered in the run event data at the conclusion of the run and logged in the experimenter's log as successful. Also logged were any events or conditions which might make the run unsuccessful (pod obscuration warnings, late pickle, loss of target lock-on, target overflight, etc). For all runs logged as successful, data printouts were ex-

amined to determine their validity. Conditions for a successful weapons release are described below.

(1) Weapon Release Conditions

(a) LGB - The following formulas were employed to calculate the maximum steering error and maximum weapon release delay that could be tolerated by the weapon seeker head. The formulas were derived from information provided by Texas Instruments, Inc., manufacturer of the GBU-10 guidance kits.

$$\text{Steering Error} \leq \text{Arc Sin} \left\{ 600 / \left[R_b - (8.0\ R_b / T_f) \cos \theta \right] \right\}$$

where

600 = 600 ft allowable azimuth error with an 8-sec weapon guidance time

R_b = Release range (ft)

T_f = Weapons time-of-fall at weapon release (sec)

θ = Aircraft pitch angle at weapon release

Weapon Release $\leq$ Computed Weapons Release + 0.7 sec.

(b) LG Maverick and LWLGM - Maximum seeker off-boresight launch limits and maximum/minimum launch ranges for the proposed LG Maverick and Sabre missile systems were implemented in the analysis. Classification of this information prevents its publication in this document.

(2) Target Tracking Requirements after Weapons Release

(a) Tracker drift tolerance when pod tracker broke lock during laser designation - 100 feet.

(b) Time tolerance when pod tracker broke lock or when pod line-of-sight became obscured during laser designation - 1 second.

(c) Target laser-designation requirements during weapon terminal guidance -- stabilized for final 2 seconds of weapon time of flight (target dependent).

(3) Laser Fire Requirements - Laser fire not interrupted more than 1 second.

When runs were questionable in this analysis, the final determination for success/failure was made in a review of the video tapes.

2.3.2.3 Other Data

Two other measures were applied to the FOV pair evaluation. Target acquisition and weapon release ranges were evaluated to determine if one of the FOV pairs provided a range advantage. The acquisition and weapon release range data were taken directly from the end-of-run data printouts. A narrow-FOV employment analysis was conducted to determine how frequently the narrow FOV was employed in each FOV pair, and for what purpose. These data were derived from a review of all runs in which a successful target acquisition was achieved and the narrow FOV was employed during the target-acquisition phase.

2.3.2.4 Field-of-Regard Data

Pod sensor gimbal angles were measured at the point of sensor line-of-sight warning onset and at the point of aircraft/stores masking or gimbal limit during each run. Both data sets were retrieved from the end-of-run data printout.

SECTION 3

DATA ANALYSIS METHODS

3.1 Subjective Data Analysis Methods

The significant effects in the pilot FOV pair ratings created by the independent variables of the study were determined by both parametric F-tests (Reference 2) and non-parametric Friedman Tests (Reference 3). Ordinarily, only non-parametric methods of analysis would be used for the analysis of subjective data. However, for the complex experiments of this study, the assumptions implicit in the non-parametric analysis methods are often violated. W. J. Conover, a non-parametric statistical advocate, concludes a discussion of the Friedman test by saying that for complex experimental situations one is practically forced to use parametric tests (Reference 4). The most appropriate parametric tests for the data after it was determined to be ordinal and normal in distribution were the F-tests. Since some statisticians may argue that the data is non-parametric from the standpoint that it is not derived from interval scale measurements, the non-parametric Friedman test was also applied to the data. Details of both tests are contained in Appendix A.

The two tests were applied to both workload and effectiveness data, with the following independent variables being common to both:

1. Subject pilots (6).

2. Field-of-view pairs (3).

3. Pod-related tasks -- workload (3), effectiveness (4).

4. Rating parameters (4) -- the rating parameters consisted of the FOV pair ratings for each experiment and "overall" FOV pair ratings completed by each pilot during the end-of-study debriefing.

For significance, the null-case hypothesis (probability that the effects due to the independent variables were random) was tested for a probability of less than or equal to 0.05 for both tests.

When the Friedman test determined significance due to an independent variable, the source of the significance was determined by employing the Friedman test between each rating condition within the independent variables. When the F-test determined significance due

to an independent variable, a T-test (Reference 2) was used to determine the source of the significance. The details of the T-test are contained in Appendix A.

Employing the F-test, significant interactions between the independent variables could be determined. For significance, the null-case hypothesis (probability that the effects due to the interactions between the independent variables were random) was tested for a probability of less than or equal to 0.05. When significance was detected, a graphical analysis was employed to determine the source of the interaction and its effect on the main effect(s).

An analysis of the pilot's comments and observations was conducted to determine a consensus of opinions about each individual field of view employed in the study and the field of regard required to deliver laser-guided ordnance.

3.2 Objective Data Analysis Methods

The objective data analysis required two separate analysis methods because of the nature of the data. The success/failure data for target acquisition and weapons delivery were discrete, whereas the time, event, and range-measurement data were continuous. Therefore, individual analysis techniques were applied to the discrete and continuous data.

3.2.1 Discrete Data

The discrete target acquisition and weapons delivery success/failure data had a very limited range due to the small number of replications performed for each data point. In addition, the small number of pilots participating in the study created a large variance in the success/failure data across the experiments. Thus, because of the small range in the data and the variance of pilot performance, the assumption of normality implicit in most statistical analysis techniques could not be made, confining the analysis to techniques which do not assume normality. The data were analyzed by use of an analysis of variance for ranked data -- the Friedman Test. With this test, the analysis was limited to determining significant effects in the data due to the following independent variables in each experiment:

1. Subject (6)
2. Field-of-View Pair (3)
3. Pop-up/REO activation Range (3).

For significance, the null-case hypothesis (probability that the effects in the success/failure data due to the independent variables were random) was tested for a probability less than or equal to 0.05.

3.2.2 Continuous Data

Because of the many empty cells in the continuous data created each time a pilot failed to acquire the target, normal statistical analysis techniques could not be applied to these data. However, a trend analysis was accomplished on the mean performance level across the pilots for each pop-up/REO activation range in each experiment to determine if these data supported the subjective results. The analysis was based on the difference between the mean performance levels and the deviation within the mean performance measures.

SECTION 4

STUDY RESULTS

4.1 Summary of Experiments

Six pilots completed 162 valid data runs in each experiment. Two pilots did not complete the study because of a facility failure. Their data, which consisted of 30 data runs accomplished in the LGB/CCRP experiment, were not used to derive the study results. This did not invalidate the experimental results since the study required only six pilots to complete the experiments and fully counterbalance the data over the experimental variables.

4.2 Subjective Data Results

4.2.1 Pilot Comments and Observations

A consensus of pilot comments and observations regarding each field of view employed in the study and the field of regard required by pilots to employ laser-guided weapons is provided in Table 4.2-1.

4.2.2 Pilot Workload Assessment

The F-test and the Friedman test determined one effect due to the independent variables. Of the four independent variables (subjects, FOV pair, task, and rating parameter), FOV pair was the single significant influencing factor on pilot workload as rated by the pilots. The mean of the pilot workload ratings for each FOV pair is depicted in Figure 4.2-1. As shown, the 6° and 1.5°, 6° and 0.86°, and 3° and 0.86° FOV pairs were rated by the pilots in an ascending order of pilot workload, respectively. The 3° and 0.86° FOV pair was obviously the highest in workload. The difference between the 6° and 1.5° and the 6° and 0.86° FOV pairs was not as obvious; however, the T-tests and the Friedman tests determined a significant difference between the pilot ratings for each FOV pair. The detailed results of the F-test, T-tests, and Friedman tests for the workload analysis are contained in Appendix B.

The F-test determined one effect due to the interaction between independent variables. This effect was due to the interaction of FOV pair by task. The graphical analysis of this interaction is depicted in Figure 4.2-2. In the 6° and 1.5° and the 6° and 0.86° FOV pairs, the pilots rated the verify-targets, fly-designation-turn, perform-complete-mission, and search-for-targets task in a descending order of relative workload. In the 3° and 0.86° FOV pair, this trend reversed, as shown in Figure 4.2-2 by the crossover between data points. However, the basic trend of rating the 6° and 1.5°,

Table 4.2-1 PILOT COMMENTS AND OBSERVATIONS

FOV	COMMENTS	SIX PILOTS
6 Deg. (Wide)	• Best for initial search/detection	• All
	• Could be employed exclusively inside 6NM against medium and large targets	• Four Pilots
	• Narrow FOV required outside 6NM	• Four Pilots
3 Deg. (Wide)	• Too narrow for initial search/detection	• All Pilots
	• Preferred for target verification and acquisition at all ranges (3-8NM); avoided FOV switching	• Three Pilots
	• Consider 3 degrees as a 3rd FOV	• Two Pilots
	• Recommend 6 degree WFOV/3 degree NFOV	• One Pilot
1.5 Deg. (Narrow)	• Best NFOV, could be employed inside 4NM for acquisition and weapon delivery	• All Pilots
0.86 Deg. ($\approx 1^{o}$ Narrow)	• Too narrow, must return to WFOV for weapon delivery	• All Pilots
	• Poor video quality	• All Pilots
Field-of-Regard	• Azimuth $\pm 180^{o}$, Elevation +30 to -90^{o}	• Three Pilots
	• Azimuth $\pm 160^{o}$, Elevation +30 to -90^{o}	• Three Pilots

SUBJECTIVE FOV WORKLOAD RATINGS

(Primary Effect)

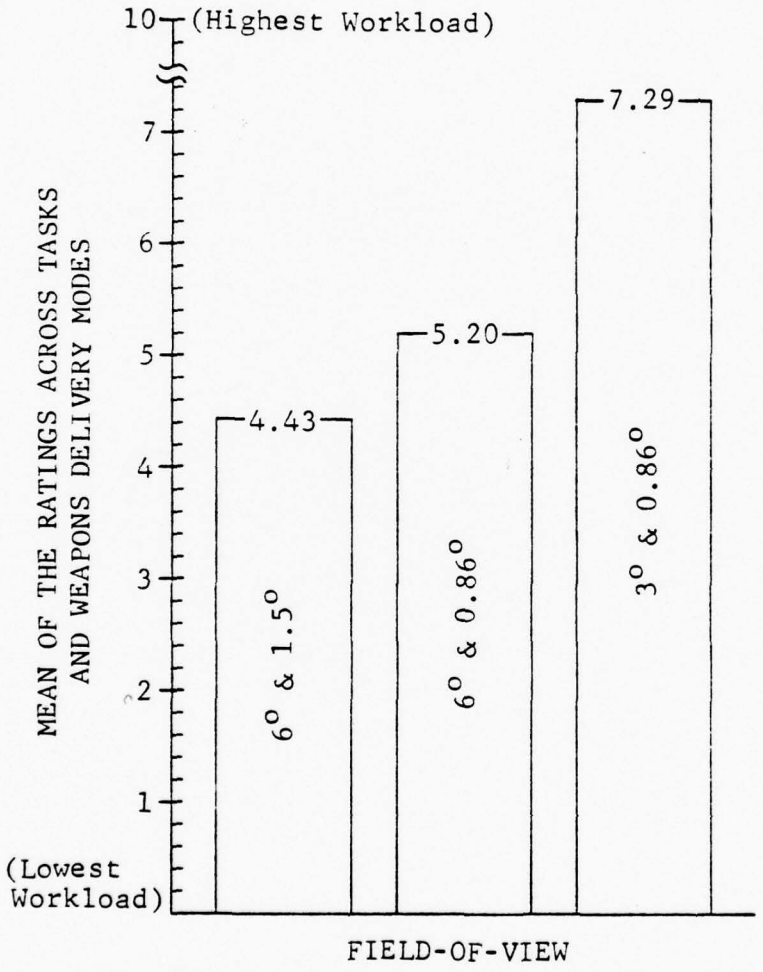

Figure 4.2-1 Pilot Workload Ratings for Each FOV Pair

SUBJECTIVE FOV WORKLOAD RATINGS BY TASK

(Secondary Effect)

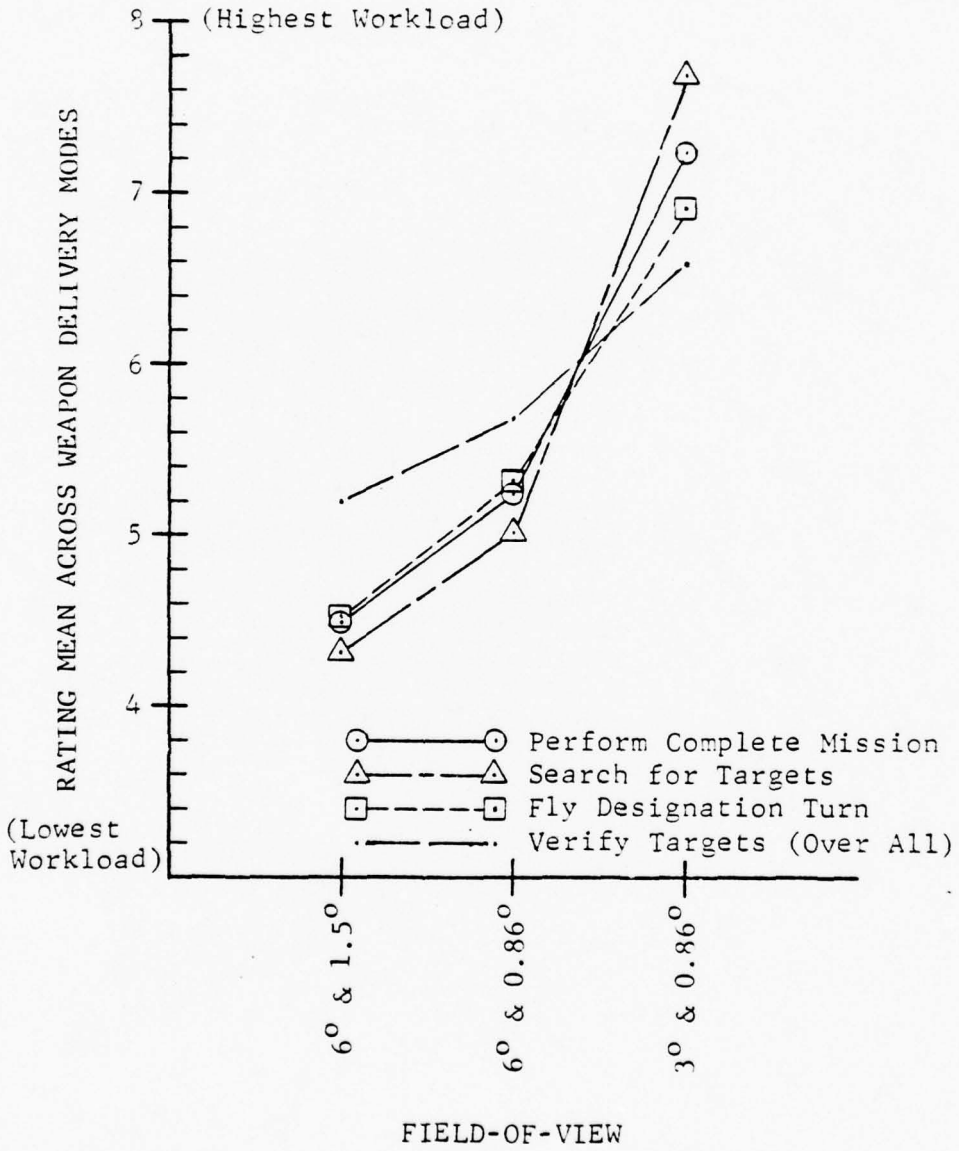

Figure 4.2-2 Graphical Analysis of the Interaction Between FOV Pair and Task in Workload Ratings

the 6^{o} and 0.86^{o}, and the 3^{o} and 0.86^{o} FOV pairs in an ascending order of relative workload for each task did not change. Therefore, the interaction between FOV pair and task variables had no confounding effect on the main effect - pilot workload by FOV pair.

The significant result of the subjective workload analysis is that the 6^{o} and 1.5^{o} FOV pair create the least pilot workload as rated by pilots.

4.2.3 Pilot Effectiveness Assessment

As in the workload analysis, the F-test and Friedman test determined one effect due to the independent variables. Again, the FOV pair variable was the single significant influencing factor on pilot effectiveness as rated by the pilots. The mean of the pilot effectiveness ratings for each FOV pair is depicted in Figure 4.2-3. As shown, the 6^{o} and 1.5^{o}, 6^{o} and 0.86^{o}, and 3^{o} and 0.86^{o} FOV pairs were rated by the pilots in a descending order of effectiveness, respectively. The 3^{o} and 0.86^{o} FOV pair was obviously lowest in effectiveness. The difference between the 6^{o} and 1.5^{o} and the 6^{o} and 0.86^{o} FOV pairs, although larger than in the workload analysis, was not as obvious; however, the T-test and Friedman tests again determined a significant difference between the pilot ratings for each FOV pair. The detained results of the F-test, T-test, and Friedman tests for the effectiveness are contained in Appendix B.

The F-test determined one effect due to the interaction between independent variables. This effect was due to the interaction of FOV pair by task. The graphical analysis of this interaction is depicted in Figure 4.2-4. As in the workload analysis, the source of the effect was due to changing trends in the order of pilot FOV pair ratings by task. This is indicated in Figure 4.2-4 by the crossover between data points. However, the basic trend of rating the 6^{o} and 1.5^{o}, the 6^{o} and 0.86^{o}, and the 3^{o} and 0.86^{o} FOV pairs in a descending order of relative effectiveness for each task did not change. Therefore, the interaction between FOV pair and task variables had no confounding effect on the main effect - effectiveness by FOV pair.

The significant result of the subjective effectiveness analysis is that the 6^{o} and 1.5^{o} FOV pair provide the most effective system as rated by pilots.

SUBJECTIVE FOV EFFECTIVENESS RATINGS

(Primary Effect)

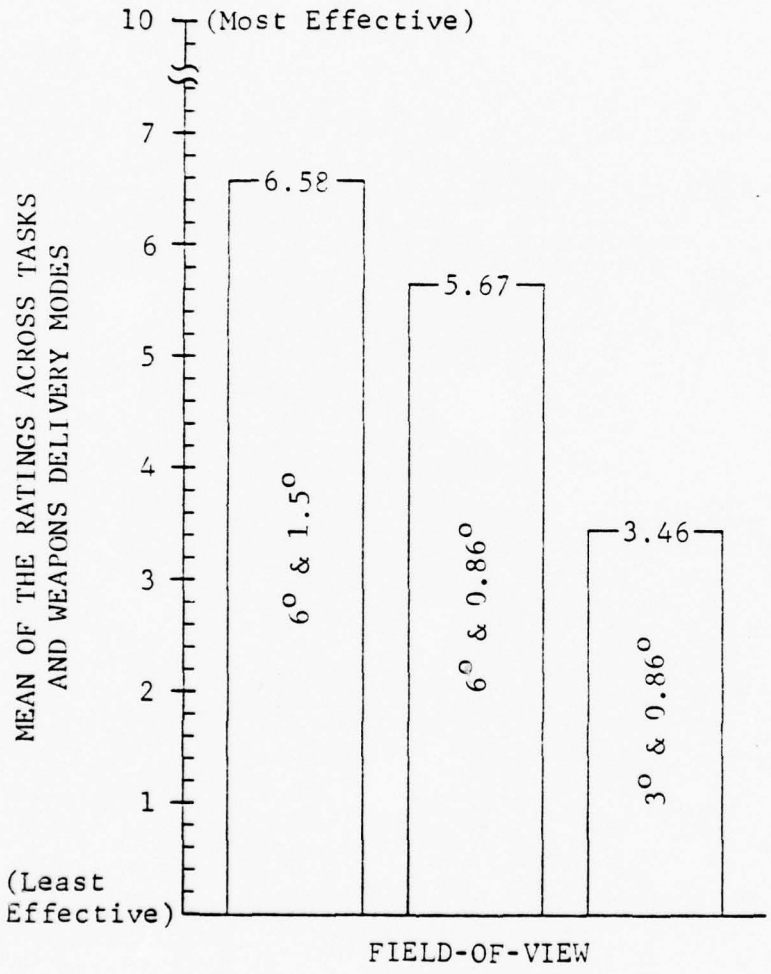

Figure 4.2-3 Pilot Effectiveness Ratings for Each FOV Pair

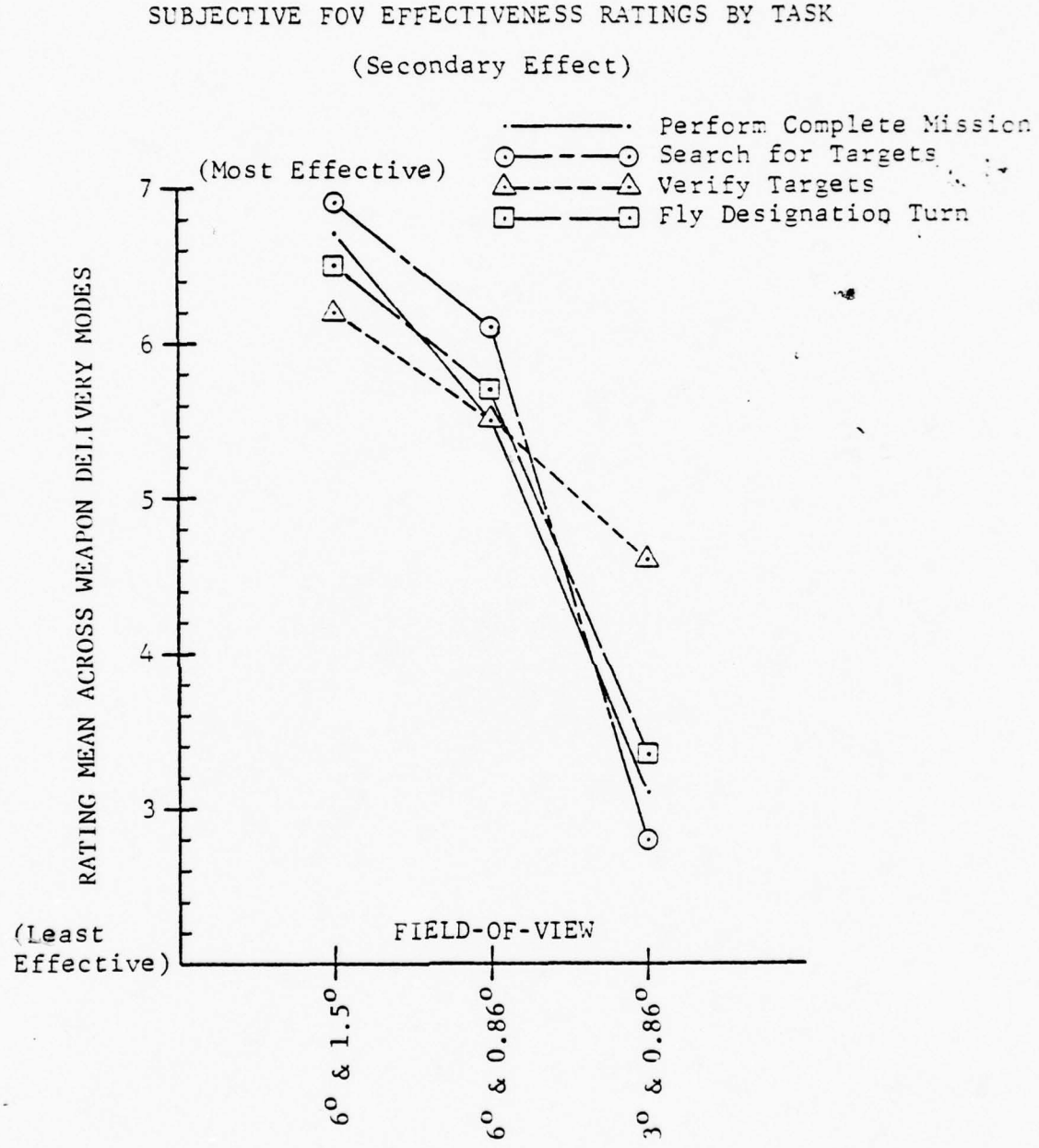

Figure 4.2-4 Graphical Analysis of the Interaction Between FOV Pair and Task in Effectiveness Ratings

4.3 Objective Data Analysis

The analysis of workload measures, effectiveness measures, acquisition and weapons delivery ranges, and narrow FOV employment was conducted on the data retrieved from each experiment.

4.3.1 LGB/CCRP Objective Results

Results of the trend analysis conducted on workload measurements are shown in Table 4.3-1. The analysis determined that the 6^{o} and 1.5^{o} FOV pair created the lowest workload in the LGB/CCRP experiment. Data from which the results were drawn are contained in Appendix B.

A summary of successful runs is contained in Table 4.3-2, which shows:

1. The number of runs in which a successful target acquisition was made out of the number of valid runs.

2. The number of runs in which a successful weapons delivery was made out of the number of runs in which a successful target acquisition was accomplished.

3. The number of runs in which a successful weapons delivery was made out of the number of runs in which a successful target acquisition was accomplished adjusted for non-pod-related weapons delivery failures.

The adjustment to the weapons delivery data was necessary because the number of non-pod-related failures did not balance over the FOV pairs. An analysis of weapon delivery failures for each FOV pair on which the adjustment was based is provided in Appendix B.

The Friedman test on the target acquisition and weapons delivery success/failure data found no significant effects due to FOV pair or pop-up/REO activation range. Appendix B contains the detailed results of these analyses.

The results of the target acquisition and weapons delivery range analyses are shown in Tables 4.3-3 and 4.3-4. Because of small differences between the mean performances and large standard deviations in these data, no significant results could be deduced from these analyses. However, it is interesting to note that, employing the 6^{o} and 1.5^{o} FOV pair, the pilots had the longest target acquisition range for all REO activation ranges and the longest weapons delivery ranges for the 6-n.mi and 3-n.mi REO activation ranges based on the mean performance levels.

Table 4.3-1 LGB/CCRP WORKLOAD TREND ANALYSIS RESULTS AND CONCLUSIONS

FOV Pair	Pod-Related Events • Slew • Designate • Change FOV			Time to Acquire/ Track Target			WORKLOAD
	REO Activation Range			REO Activation Range			
	6NM	4.5NM	3NM	6NM	4.5NM	3NM	
6° & 1.5°	Fewest	Fewest	No Significant Difference	Least	Least	Least	(Lowest)
6° & 0.86°	Most	Fewest		Most	Least	—	—
3° & 0.86°	—	Most		—	Most	Most	Highest

Table 4.3-2 LGB/CCRP SUCCESSFUL RUN SUMMARY

FOV Pair	6° & 1.5°			6° & 0.86°			3° & 0.86°		
REO Range	6NM	4.5NM	3NM	6NM	4.5NM	3NM	6NM	4.5NM	3NM
Acquisition Success	17/18	16/18	13/18	16/18	16/18	16/18	15/18	16/18	12/18
Acquisition Success Over All	46/54 85%			48/54 89%			43/54 80%		
Weapon Delivery Success	10/17	12/16	8/13	13/16	12/16	13/16	11/15	11/16	10/12
Weapon Delivery Success Over All	30/46 65%			38/48 79%			32/43 74%		
Adjusted Delivery Success Over All	30/38 79%			38/45 84%			32/39 82%		

Table 4.3-3 LGB/CCRP TARGET ACQUISITION
RANGE ANALYSIS RESULTS

FOV	6° & 1.5°			6° & 0.86°			3° & 0.86°		
REO RANGE	6NM	4.5NM	3NM	6NM	4.5NM	3NM	6NM	4.5NM	3NM
n	15	16	13	16	16	16	14	16	12
$\overline{X}$	28,782 ft.	21,525 ft.	15,081 ft.	24,696 ft.	21,499 ft.	14,415 ft.	27,337 ft.	20,302 ft.	14,815 ft.
S	5,997 ft.	3,892 ft.	2,301 ft.	5,951 ft.	4,171 ft.	2,086 ft.	4,861 ft.	4,335 ft.	2,014 ft.

Table 4.3-4 LGB/CCRP WEAPONS DELIVERY
RANGE ANALYSIS RESULTS

FCV	6^{o} & 1.5^{o}			6^{o} & 0.86^{o}			3^{o} & 0.86^{o}		
REO RANGE	6NM	4.5NM	3NM	6NM	4.5NM	3NM	6NM	4.5NM	3NM
n	14	16	13	15	15	16	13	16	12
$\bar{X}$	18,277 ft.	14,926 ft	11,565 ft	17,447 ft	15,846 ft	11,082 ft	17,822 ft	14,379 ft	10,897 ft
S	3,457 ft	4,357 ft	1,669 ft	3,998 ft	2,861 ft	1,662 ft	4,331 ft	3,381 ft	2,103 ft

The narrow-FOV analysis for the LGB/CCRP experiment is shown in Table 4.3-5. The frequency of narrow-FOV utilization was approximately the same in the FOV pairs employing the 6^{o} wide FOV and almost non-existant for the FOV pair employing the 3^{o} wide FOV. Significant narrow-FOV usage for target acquisition was confined to the 1.5^{o} FOV.

Table 4.3-5 LGB/CCRP NARROW FOV EMPLOYMENT ANALYSIS RESULTS

FOV	6^o & 1.5^o			6^o & 0.86^o			3^o & 0.86^o		
REO RANGE	6NM	4.5NM	3NM	6NM	4.5NM	3NM	6NM	4.5NM	3NM
No. of Runs WFOV Used	15	16	13	16	16	16	14	16	12
No. of Runs NFOV Used	7	5	1	7	2	1	2	0	0
% of Runs NFOV Used	47%	31%	8%	44%	12.5%	6%	13%	0%	0%
% of Runs NFOV Used for Tgt. Acq.	6/15 40%	4/16 25%	1/13 8%	1/16 6%	1/16 6%	1/16 6%	1/14 7%	0/16 0%	0/12 0%

NOTE: Pilots always began run in wide FOV.

4.3.2 LG Maverick/LGM Objective Results

Results of the trend analysis conducted on workload measures are shown in Table 4.3-6. The analysis determined that the 6° and 1.5° FOV pair created the lowest workload in the LG Maverick/LGM experiment. Data from which the results were drawn are contained in Appendix B.

A summary of successful runs is contained in Table 4.3-7. The weapons delivery success rates were again adjusted to remove the non-pod-related failures due to an uneven distribution of those failures over the FOV pairs. An analysis of the weapon delivery failures on which the adjustment was based is provided in Appendix B.

The results of the target acquisition and weapons delivery range analysis are shown in Tables 4.3-8 and 4.3-9. Again, the relatively small difference between the mean performance levels and the large standard deviations in the target acquisition data made it impossible to deduce any significant results from the analysis. However, it is interesting to note that the pilots had the longest target acquisition range and over all REO activation ranges while employing the 6° and 1.5° and the 3° and 0.86° FOV pairs. The weapon release analysis determined a significant result. For the two longest REO activation ranges, REO activation at run initiation (ARI) and at 6 n.mi, the pilots launched the Maverick at significantly longer ranges while employing the 6° and 1.5° and the 3° and 0.86° FOV pairs.

The narrow-FOV employment analysis for the LG Maverick/LGM is shown in Table 4.3-10. The frequency of narrow-FOV utilization was approximately the same in the FOV pairs employing the 6° wide FOV. In the 3° and 0.86° FOV pair, the frequency of narrow-FOV utilization was high (86% of the runs) for the longest REO activation range but decreased to 37.5% for the intermediate range and was non-existent for the short REO activation range. Narrow-FOV usage for target acquisition was significantly higher in the 1.5° FOV over all REO activation ranges.

Table 4.3-6 LG MAVERICK/LGM WORKLOAD TREND ANALYSIS RESULTS AND CONCLUSIONS

FOV Pair	Pod-Related Events • Slew • Designate • Change FOV			Time to Acquire/ Track Target			WORKLOAD
	REO Activation Range			REO Activation Range			
	ARI	6NM	4NM	ARI	6NM	4NM	
6^{o} & 1.5^{o}	Fewest	—	Fewest	Least	—	Least	(Lowest)
6^{o} & 0.86^{o}	—	Most	Most	—	Most	—	Highest
3^{o} & 0.86^{o}	Most	Fewest	—	Most	Least	Most	—

Table 4.3-7 LG MAVERICK/LGM SUCCESSFUL RUN SUMMARY

FOV Pair	6° & 1.5°			6° & 0.86°			3° & 0.86°		
REO Range	ARI	6NM	4NM	ARI	6NM	4NM	ARI	6NM	4NM
Acquisition Success	15/18	18/18	18/18	16/18	17/18	18/18	14/18	16/18	13/18
Acquisition Success Over All	51/54 94%			51/54 94%			43/54 80%		
Weapon Delivery Success	12/15	10/18	12/18	14/16	12/17	14/18	13/14	15/16	10/13
Weapon Delivery Success Over All	34/51 67%			40/51 78%			38/43 88%		
Adjusted Delivery Success Over All	34/40 85%			40/47 85%			38/41 93%		

Table 4.3-8 LG MAVERICK/LGM TARGET ACQUISITION
RANGE ANALYSIS RESULTS

FOV	6^{o} & 1.5^{o}			6^{o} & 0.86^{o}			3^{o} & 0.86^{o}		
REQ RANGE	ARI	6NM	4NM	ARI	6NM	4NM	ARI	6NM	4NM
n	15	18	18	16	17	18	14	16	13
$\bar{X}$	36778 ft	25328 ft	17491 ft	34917 ft	23263 ft	17024 ft	39329 ft	27314 ft	18528 ft
S	8242 ft	8394 ft	4219 ft	13619 ft	6690 ft	4778 ft	12148 ft	3706 ft	4055 ft

Table 4.3-9 LG MAVERICK/LGM WEAPONS DELIVERY
RANGE ANALYSIS RESULTS

FOV	6^o & 1.5^o			6^o & 0.86^o			3^o & 0.86^o		
REQ RANGE	ARI	6NM	4NM	ARI	6NM	4NM	ARI	6NM	4NM
n	15	15	16	16	17	16	14	16	13
$\bar{X}$	27398 ft	23984 ft	15738 ft	22670 ft	20800 ft	15693 ft	28625 ft	23592 ft	16258 ft
S	5871 ft	5501 ft	3342 ft	7697 ft	6677 ft	3777 ft	2980 ft	3777 ft	3859 ft

Table 4.3-10 LG MAVERICK/LGM NARROW FOV EMPLOYMENT ANALYSIS RESULTS

FOV	6^{o} & 1.5^{o}			6^{o} & 0.86^{o}			3^{o} & 0.86^{o}		
REO RANGE	ARI	6NM	4NM	ARI	6NM	4NM	ARI	6NM	4NM
No. of Runs WFOV Used	15	18	18	16	17	18	14	16	13
No. of Runs NFOV Used	15	13	8	16	14	7	12	6	0
% of Runs NFOV Used	100%	72%	44%	100%	82%	38%	86%	37.5%	0%
% of Runs NFOV Used for Tgt. Acq.	15/15 100%	13/18 72%	6/18 33%	10/16 62.5%	8/17 47%	3/18 17%	6/14 43%	4/16 25%	0/13 0%

NOTE: Pilots always began run in wide FOV.

4.3.3 LWLGM/LGMDT Objective Results

Results of the trend analysis conducted on workload measures are contained in Table 4.3-11. At one pop-up range point for the 6^{o} and 1.5^{o} FOV pair there was insufficient successful runs to make a valid workload determination. The analysis shows both the 6^{o} and 1.5^{o} and the 6^{o} and 0.86^{o} FOV pairs to be lowest in workload, with no significant difference existing between the two for those data points with sufficient data to make a determination. Data from which the results were drawn are contained in Appendix B.

A summary of successful runs is contained in Table 4.3-12. The weapon delivery successes have been adjusted to remove the non-pod-related failures. A comparatively high target-acquisition failure rate existed for all FOV pairs in this experiment. A target-acquisition failure analysis was performed to determine the cause of the high failure rate. The analysis determined that 61 of the 78 failures to acquire the target were due to pilots not locating the target area visually on the wind screen display with sufficient time to locate the targets and to lock the pod on. The results of the failure analysis are contained in Table 4.3-13. The high target-acquisition failure rates were therefore not related to the EO pod. Instead, the failures were related to the pilot's inability to employ the windscreen display to navigate and locate the target area heads-up. Since the target acquisition success/failure data did not relate to the EO pod, this measure was not analyzed to determine system effectiveness.

The Friedman test on the weapons delivery success/failure data found no significant effects due to FOV pair or pop-up range. The detailed results of these analysis are given in Appendix B.

The target acquisition range data did not reflect the pilots' capability to employ the pod to search and acquire targets. Instead, it indicated where the pilots located the target area visually, head-up on the windscreen display. Since weapon delivery range was dependent on target acquisition range, the weapon delivery range data did not reflect the pilot's ability to employ the EO pod to deliver a weapon. Therefore, the range data analyses contained in Appendix B for the LWLGM/LGMDT are not representative of the pilots' capability to employ the EO pod to acquire a target or deliver a missile.

The narrow-FOV employment analysis for the LWLGM/LGMDT experiment is shown in Table 4.3-14. The narrow FOVs were used significantly more often in the FOV pairs employing the 6^{o} wide FOV. Narrow-FOV usage for target acquisition was significantly higher in the 1.5^{o} narrow-FOV over all pop-up range points.

Table 4.3-11 LWLGM/LGMDT WORKLOAD TREND ANALYSIS
RESULTS AND CONCLUSIONS

FOV Pair	Pod-Related Events • Slew • Designate • Change FOV			Time to Acquire/ Track Target			WORKLOAD
	Pop-Up Range			Pop-Up Range			
	7NM	5.5NM	4NM	7NM	5.5NM	4NM	
6° & 1.5°	Fewest	X	No Significant Difference	Least	X	Least	No Significant Difference
6° & 0.86°	Fewest	Fewest		—	Least	Least	
3° & 0.86°	Most	Most		Most	Most	Most	Highest

X- Insufficient Successful Runs to make Determination

NOTE: Pilots always began run in wide FOV.

Table 4.3-12 LWLGM/LGMDT SUCCESSFUL RUN SUMMARY

FOV Pair	6° & 1.5°			6° & 0.86°			3° & 0.86°		
REO Range	7NM	5.5NM	4NM	7NM	5.5NM	4NM	7NM	5.5NM	4NM
Acquisition Success	11/18	5/18	8/18	10/18	13/18	7/18	13/18	8/18	10/18
Acquisition Success Over All	24/54 44%			30/54 55%			31/54 57%		
Weapon Delivery Success	11/11	5/5	7/8	6/10	10/13	6/7	12/13	8/8	9/10
Weapon Delivery Success Over All	23/24 96%			22/30 73%			29/31 94%		
Adjusted Delivery Success Over All	23/23 100%			22/26 85%			29/30 97%		

Table 4.3-13 TARGET ACQUISITION FAILURE ANALYSIS RESULTS

NON-POD RELATED FAILURES	POD RELATED FAILURES
6^{o} and 1.5^{o} FOV Pair	
20 - No Acquisitions (pilots lost and never found target area)	3 - Target Misidentifications
4 - Late Acquisitions (pilots located target too late to achieve a valid missile launch)	1 - Crash before Target Acquisition (Pilot glued to REO display)
1 - Switchology Problem (pilot failed to select missile)	
6^{o} and 0.86^{o} FOV Pair	
14 - No Acquisitions	5 - Target Misidentifications
4 - Late Acquisitions	2 - Crashes before Target Acquisition
3^{o} and 0.86^{o} FOV Pair	
14 - No Acquisitions	3 - Target Misidentifications
5 - Late Acquisitions	
1 - Switchology Problem	

Table 4.3-14 LWLGM/LGMDT NARROW FOV EMPLOYMENT ANALYSIS RESULTS

FOV	6° & 1.5°			6° & 0.86°			3° & 0.86°		
POP-UP RANGE	7NM	5.5NM	4NM	7NM	5.5NM	4NM	7NM	5.5NM	4NM
No. of Runs WFOV Used	11	5	8	10	13	7	13	8	10
No. of Runs NFOV Used	9	2	3	5	5	1	6	2	0
% of Runs NFOV Used	82%	40%	37%	50%	39%	14%	46%	25%	0%
% of Runs NFOV Used for Tgt. Acq.	8/11 73%	1/5 20%	1/8 12.5%	1/10 10%	2/13 15%	0/7 0%	1/13 8%	0/8 0%	0/10 0%

4.4 Field-of-Regard Results

The seeker field-of-regard requirements were evaluated through an analysis of pod-sensor line-of-sight warning and obscuration data. Pod-sensor line-of-sight warnings and obscurations occurred predominantly in the LGB/CCRP experiment. As an example of the dominance, 90 obscurations occurred in the LGB/CCRP experiment, 12 in the LG Maverick/LGM experiment, and none in the LWLGM/LGMDT experiment. Therefore, only the data obtained from the LGB/CCRP experiment were analyzed.

4.4.1 Pod Sensor Line-of-Sight Warning Results

A total of 255 pod-sensor line-of-sight warnings occurred in 116 of 162 valid runs. Figure 4.4-1 shows the warning onset implemented for the study and the number of warning occurences by 10-degree azimuth increments. Of the 255 warnings, 128 were due to aircraft or stores masking and 127 were due to pod-sensor gimbal limits. Of the 128 warnings due to aircraft or stores masking, 79 (62%) occurred between -10 and -50 degrees of azimuth. An analysis of the aircraft attitude at these warnings determined that the warnings were due to excessive left roll induced by the pilots immediately following bomb release while the aircraft was pitched up greater than 10 degrees for a toss maneuver. Roll to the right under the same conditions did not create the same effect because the greater field-of-regard with the pod mounted on the right side of the aircraft inlet.

4.4.2 Pod Sensor Line-of-Sight Obscuration Results

A total of 90 pod-sensor line-of-sight obscurations occurred out of the 255 pod-sensor line-of-sight warnings. The 90 obscurations occurred in 73 runs. Figure 4.4-2 shows the obscuration limits implemented for the study and the number of obscuration occurrences by 10-degree increments. Of the 90 obscurations, 41 (45%) were due to pod-seeker gimbal limits and 49 (55%) were due to aircraft or stores masking. Again, the major portion (70%) of the obscurations due to aircraft and stores masking occurred between -10 and -50 degrees of azimuth.

4.4.3 Pod Gimbal Limit Analysis and Results

The pod-sensor gimbal angles and aircraft ground track from weapon release to weapon impact for a typical LGB delivery in which the simulated pod-sensor gimbal limits were reached are shown in Figure 4.4-3. Of specific interest during the delivery are the aircraft ground track and pod-sensor gimbal angles from 15 seconds to 20 seconds after bomb release. During this period the

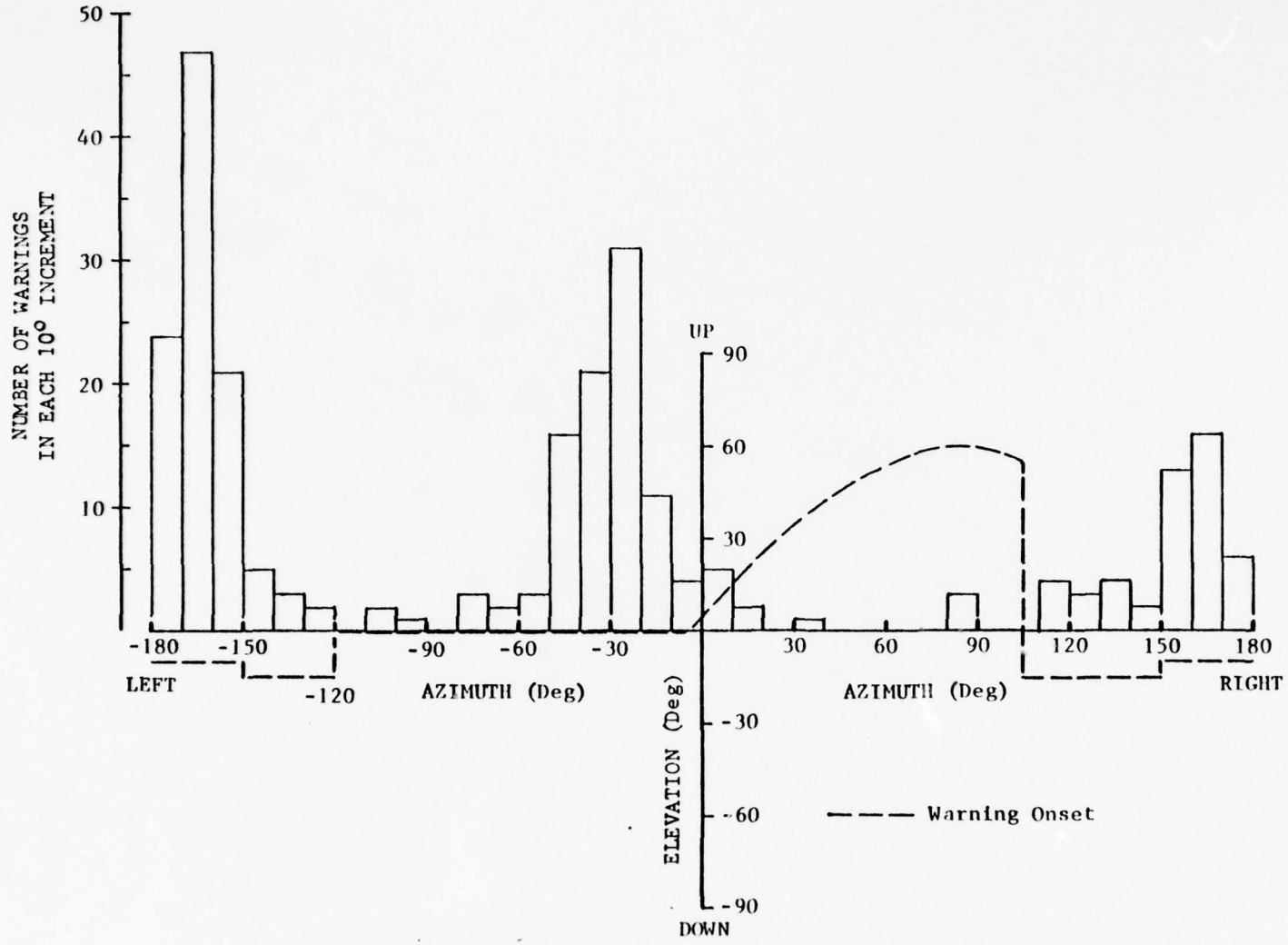

Figure 4.4-1 Warning Onset and Number of Warnings by 10° Increments

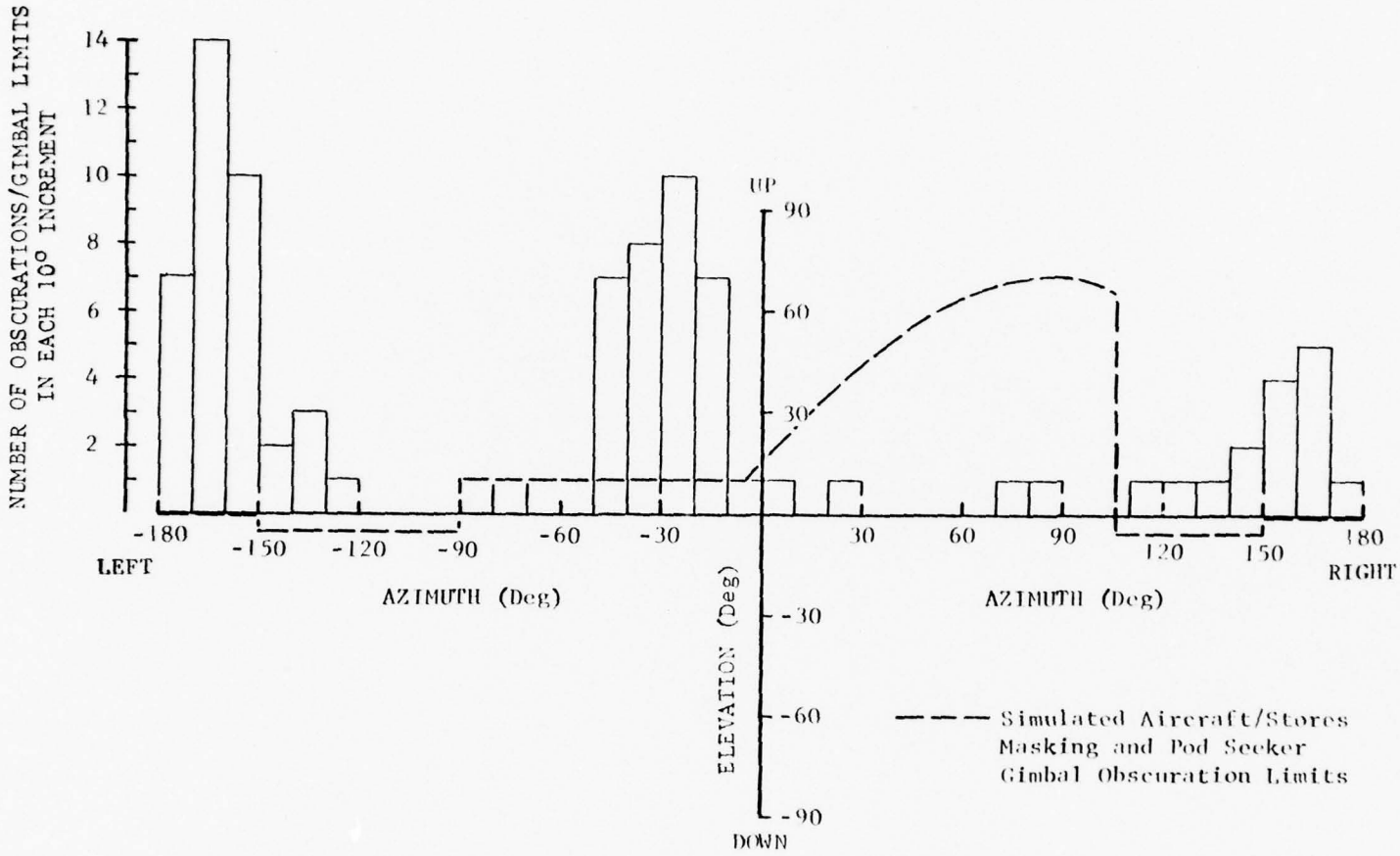

Figure 4.4-2 Obscuration Limits and Number of Obscurations by 10° Increments

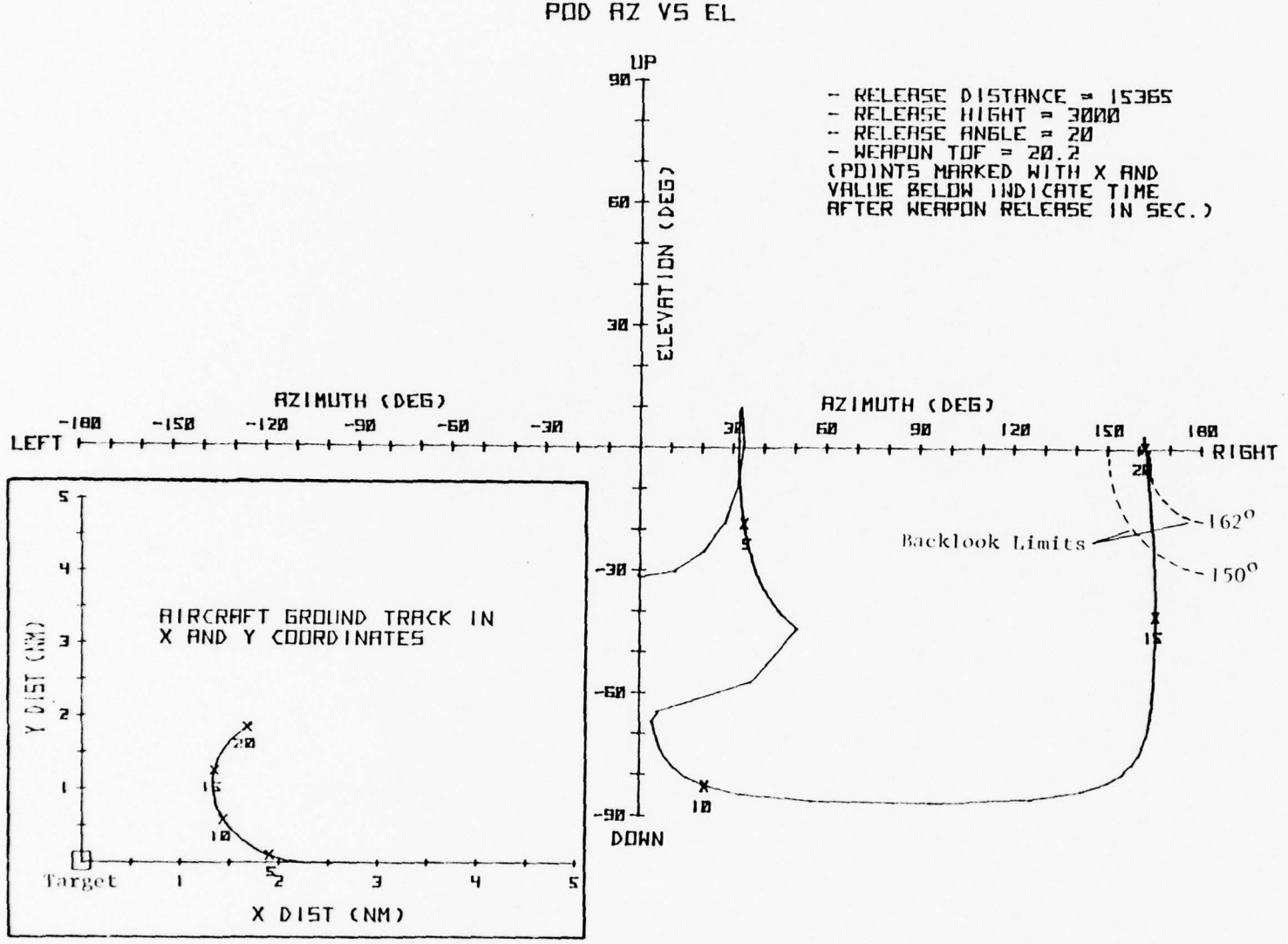

Figure 4.4-3 Pod Sensor Gimbal Angles and Aircraft Ground Track for a Typical LGB Delivery

the aircraft's longitudinal axis (tail of the aircraft) is passing through the target, which is at the origin of the X and Y axes. When this occurs, the pod gimbal translation is almost totally in the elevation axis, as indicated by the vertical movement of the line describing the pod gimbal angles.

Because of this phenomenon, the simulated pod-sensor gimbal limits were defined between 150 and 180 degrees of azimuth at zero elevation to detect the azimuth angle at which the pod gimbal intersected the zero elevation line (azimuth axis). The azimuth angle at the zero elevation line provided an approximation of the pod-seeker gimbal back-look requirement to contain the excursion. This is shown in Figure 4.4-3, where pod gimbal back-look limits of 150 and 162 degrees are shown on the right-hand side of the azimuth axis by dashed lines. Note that the line describing the pod gimbal translation clearly violates the 150-degree back-look limit and that the 162-degree back-look limit is not violated since the line is running tangent to the limit. Also note that the line describing the pod gimbal translation crosses the zero elevation line (azimuth axis) at approximately 162 degrees.

The point at which the line describing the pod gimbal translation begins its vertical climb and crosses the azimuth axis is dependent on aircraft altitude above the target and aircraft pitch and roll in the turn. In the LGB/CCRP experiment the point at which the line began its vertical climb, thus creating pod gimbal limit warnings and limit broaches, was almost totally dependent on aircraft altitude above the target. This was primarily due to the canned scenario employed in the study. If the pilot had sufficient altitude when a gimbal limit warning occurred he could duck under the gimbal limit by rolling the aircraft level and pushing the nose down.

Three techniques for measuring the required pod-sensor gimbal limits were considered: (1) defining gimbal look-back limits and measuring the frequency that each limit was used during the run, (2) defining gimbal look-back limits and measuring the frequency that each limit was used when the pilots reached a simulated pod gimbal limit warning, and (3) defining gimbal look-back limits and measuring the frequency each limit was used when the simulated gimbal limits were reached. The first technique was not used since the pilots could have reached a gimbal limit defined for analysis without warning. In 81 instances of 127 pod gimbal limit warnings, the pilot had sufficient altitude and time available to avoid simulated gimbal limit and possibly the gimbal limits defined for analysis, therefore, the second technique was not appropriate. The simulated gimbal limit was reached because the pilot was either distracted by workload and did not react quickly enough to avoid

the simulated gimbal limit or did not have sufficient altitude to escape the gimbal limit. In either case the pilot would not have avoided gimbal limits defined for analysis. Therefore, the third technique was chosen as the method for analysis.

The pod sensor gimbal limits for analysis were defined in 10-degree increments from 150 to 180 degrees of azimuth. The frequency that each limit was used when the simulated gimbal limits were reached is graphically portrayed in Figure 4.4-4.

There were 100 successful runs in the LGB/CCRP experiment. Twelve runs were scored unsuccessful because of a pod-sensor line-of-sight obscuration which lasted more than 1 second. Eight obscurations were due to pod sensor gimbal limits, and four obscurations were due to aircraft/stores masking. Since the 1-second criteria for determining run success or failure was arbitrary for pod sensor gimbal limits, a further analysis of the successful runs, including the eight failures due to pod-sensor gimbal limits, was conducted. For the analysis, pod-sensor back-look angles of 150, 150, 170, and 180 degrees were defined, and the percentage of the 108 runs in which the gimbal limit had no factor (was not reached) was determined. The results of this analysis are displayed in Figure 4.4-4 to provide a better picture of pod sensor gimbal limits in the context of run success.

The frequency analysis of gimbal limit usage determined that the highest frequency occurred between pod-sensor gimbal back-look angles of 160 and 170 degrees. The analysis of successful runs determined that from 75% to 95% of the successful runs did not have obscurations due to gimbal limits when the gimbal limits were defined between 160 and 170 degrees.

4.5 Summary of Results

4.5.1 Subjective Results

The analysis of pilot ratings employing both a parametric F-test and a non-parametric Friedman test determined that the 6^{o} and 1.5^{o} FOV pair provided the least pilot workload and the most system effectiveness.

4.5.2 Objective Results

The trend analysis of workload measures from the three experiments determined that the 6^{o} and 1.5^{o} FOV pair provided the lowest workload. In the LWLGM/LGMDT experiment, no significant difference existed between the 6^{o} and 1.5^{o} and the 6^{o} and 0.86^{o} FOV pairs. In the two other experiments, a significant difference occurred between each FOV pair.

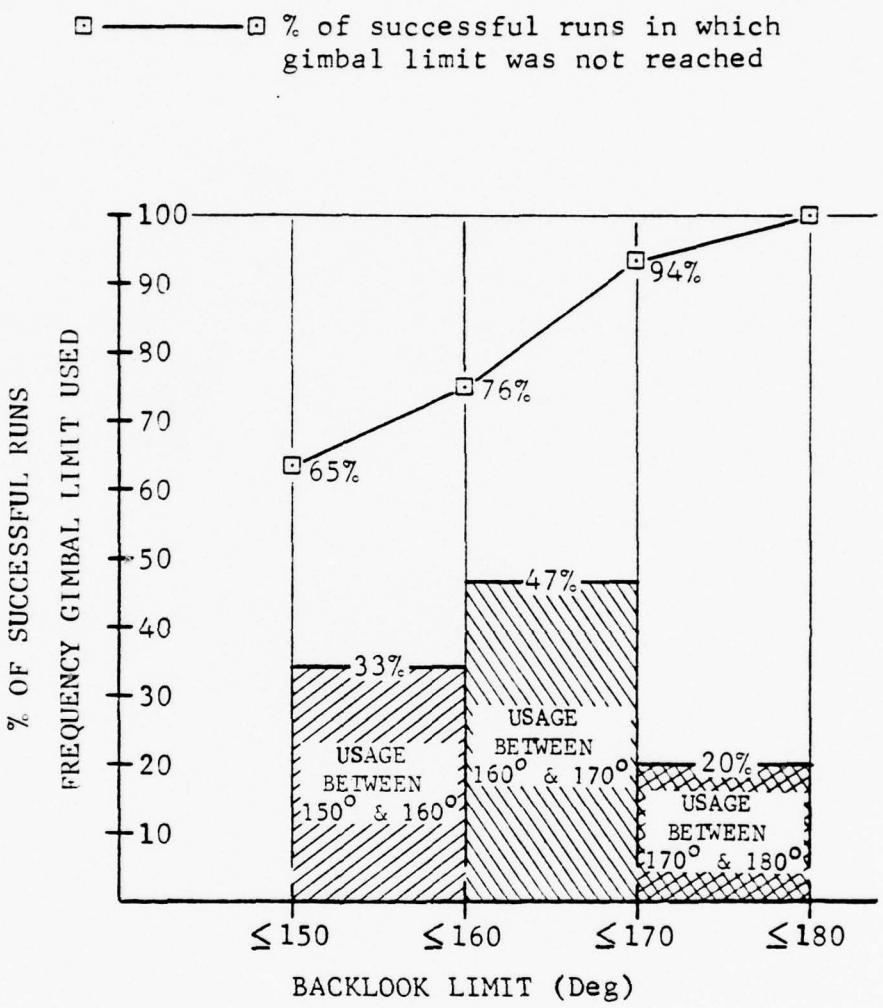

Figure 4.4-4 Pod Sensor Gimbal Limit Analyses

The analysis of effectiveness measures did not determine any significant difference between FOV pairs.

Because of small differences between the mean performance levels and because of large standard deviations in the data, only one significant result could be deduced from the target-acquisition and weapon-release range measures. The result occurred in the LG Maverick/LGM experiment where pilots employing the 6° and 1.5° and the 3° and 0.86° FOV pairs obtained significantly longer weapons release ranges than when employing the 6° and 0.86° FOV pair. However, the trends in these data supported the subjective results in all instances.

The narrow-FOV utilization analysis determined that the narrow FOV was employed significantly more often in the FOV pairs having the 6° wide FOV. Narrow-FOV usage for target acquisition was significantly higher in the 1.5° narrow FOV over all experiments.

SECTION 5

CONCLUSIONS

5.1 Individual Fields-of-View

Conclusions concerning each individual field-of-view are based on pilot remarks and observations, pilot field-of-view pair ratings, and objective experimental measures. These conclusions are discussed below.

5.1.1 6-Degree Wide FOV

When employed for target search, the 6° FOV provided excellent capability at all ranges against all targets. When employed for target verification against large fixed targets, the 6° FOV was good at medium to close ranges; however, against small mobile-type targets, it was limited to close ranges. When employed for target lock-on against large targets, the 6° FOV was good at all ranges; however, against small targets it was limited to medium to close ranges.

5.1.2 3-Degree Wide FOV

The 3° FOV was too narrow for target search operations at attack ranges simulated in the study. However, for target verification and lock-on operations, the 3° FOV provided a good capability at all ranges against all targets.

5.1.3 1.5-Degree Narrow FOV

The 1.5° FOV was too narrow for target search operations at all ranges. The 1.5° FOV provided an excellent capability for target verification at all ranges. Target lock-on employing the 1.5° FOV was good at all ranges against small targets; however, it was limited to long and medium ranges for large fixed targets.

5.1.4 0.86-Degree Narrow FOV

The 0.86° FOV with degraded video clarity was too narrow for the attack ranges simulated. Although the pilots were briefed on the degraded video and shown a video tape of an EO Pod flight demonstration containing profiles employing 1° and $\frac{1}{2}^{\circ}$ FOVs with excellent video quality prior to the experiments, some bias did occur as a result of the poor video quality. The amount of bias introduced by the degraded video in this FOV on the subjective pilot ratings and objective performance levels was impossible to determine.

5.2 Field-of-View Pairs

From analysis of the primary data source, the subjective pilot field-of-view ratings, it was determined that the 6° and 1.5° FOV pair provided the least pilot workload and the most system effectiveness. The significant results from the analysis of the secondary data source, objective pilot performance measures, supported the primary data source. Therefore, for the simulated attack scenario, which included:

- Low-altitude (500 feet), high-speed (540 KTAS) ingress
- Pop-up for target acquisition and weapons delivery
- Visibility restrictions ranging between 6 and 3 n.mi
- A weather ceiling of 2500 feet

and for the simulator limitations, which included:

- Degraded video clarity in the 0.86° FOV
- A 50-degree (measured diagonally) forward visibility provided by a 500-line, black and white video monitor
- A terrain board measuring 80 ft by 40 ft that, at 1200-to-1 scale, provided a working area of 14 n.mi by 7 n.mi

the 6° and 1.5° FOV pair is best.

5.3 Pod Seeker Field-of-Regard

The results of the pod-sensor line of sight warning and pod-sensor line-of-sight obscuration analyses indicated that the pilots responded well to the warning tone. Of the 255 warnings, only 90 resulted in pod-sensor line-of-sight obscurations or gimbal limits. These results indicate the need for a warning implementation in aircraft carrying an advanced EO pod.

The results of the pod-sensor gimbal limit analysis indicate a gimbal back-look capability defined between 160 and 170 degrees is required for the delivery of laser guided bombs.

REFERENCES

1. F-16 Advanced Electro-Optical Pod Field-of-View Study Flight Test Plan, FZM-6781, General Dynamics, Fort Worth, Texas, 1978.

2. Cochran, W. G. and Cox, G. M., Experimental Designs, Chapter 3, New York: John Wiley and Sons, Incorporated, 1957.

3. Winer, B. J., Statistical Principles in Experimental Design, Chapter 4 and Appendix A, New York: McGraw-Hill Book Company, Incorporated, 1962.

4. Conover, W. J., Practical Nonparametric Statistics, p. 274, New York: John Wiley and Sons, Incorporated, 1971.

APPENDIX A

F-TEST, T-TEST, AND FRIEDMAN TEST FORMULAS

DETAILS OF F-TEST APPLIED TO PILOT WORKLOAD RATINGS

	SOURCE	DEGREES OF FREEDOM	ESTIMATED MEAN SQUARE	F-TEST
1	Subjects (A)	5	$27\sigma^2_A$	None
2	Mode (B)	3	$54\tau^2_B + 9\sigma^2_{AB}$	(2) ÷ (5)
3	Field of View (C)	2	$54\tau^2_C + 9\sigma^2_{AC}$	(3) ÷ (6)
4	Task (D)	2	$54\tau^2_D + 9\sigma^2_{AD}$	(4) ÷ (7)
5	A X B	15	$9\sigma^2_{AB}$	None
6	A X C	10	$9\sigma^2_{AC}$	None
7	A X D	10	$9\sigma^2_{AD}$	None
8	B X C	6	$18\tau^2_{BC} + 3\sigma^2_{ABC}$	(8) ÷ (11)
9	B X D	6	$18\tau^2_{BD} + 3\sigma^2_{ABD}$	(9) ÷ (12)
10	C X D	4	$18\tau^2_{CD} + 3\sigma^2_{ACD}$	(10) ÷ (13)
11	A X B X C	30	$3\sigma^2_{ABC}$	None
12	A X B X D	30	$3\sigma^2_{ABD}$	None
13	A X C X D	20	$3\sigma^2_{ACD}$	None
14	B X C X D	12	$6\tau^2_{BCD} + \sigma^2_{ABCD}$	(14) ÷ (15)
15	A X B X C X D	60	σ^2_{ABCD}	None
	TOTAL	215		

DETAILS OF F-TEST APPLIED TO PILOT EFFECTIVENESS RATINGS

	SOURCE	DEGREES OF FREEDOM	ESTIMATED MEAN SQUARE	F-TEST
1	Subjects (A)	5	$48\sigma^2_A$	None
2	Mode (B)	3	$72\tau^2_B + 12\sigma^2_{AB}$	(2) ÷ (5)
3	Field of View (C)	2	$96\tau^2_C + 16\sigma^2_{AC}$	(3) ÷ (6)
4	Task (D)	3	$72\tau^2_D + 12\sigma^2_{AD}$	(4) ÷ (7)
5	A X B	15	$12\sigma^2_{AB}$	None
6	A X C	10	$16\sigma^2_{AC}$	None
7	A X D	15	$12\sigma^2_{AD}$	None
8	B X C	6	$24\tau^2_{BC} + 4\sigma^2_{ABC}$	(8) ÷ (11)
9	B X D	9	$18\tau^2_{BD} + 3\sigma^2_{ABD}$	(9) ÷ (12)
10	C X D	6	$24\tau^2_{CD} + 4\sigma^2_{ACD}$	(10) ÷ (13)
11	A X B X C	30	$4\sigma^2_{ABC}$	None
12	A X B X D	45	$3\sigma^2_{ABD}$	None
13	A X C X D	30	$4\sigma^2_{ACD}$	None
14	B X C X D	18	$6\tau^2_{BCD} + \sigma^2_{ABCD}$	(14) ÷ (15)
15	A X B X C X D	90	σ^2_{ABCD}	None
	TOTAL	287		

T-TEST

The t value was calculated using the following method.

1. The appropriate standard deviation for the denominator of the t-test was estimated by:

   a. Estimating σ^2_x from the Mean Square used as a denominator in the F-test.

   b. Estimating $\sigma^2_{\bar{x}}$ by:

   $$\sigma^2_{\bar{x}} = \frac{\sigma^2_x}{\sqrt{n}}$$ where n = Number of Observations in the Mean

   c. Estimating $\sigma^2_{\bar{x}_1 - \bar{x}_2}$ by:

   $$\sigma^2_{\bar{x}_1 - \bar{x}_2} = 2\,\sigma^2_{\bar{x}}$$

   d. The demoninator was then determined by:

   $$S_{\bar{x}_1 - \bar{x}_2} = \sqrt{\sigma^2_{\bar{x}_1 - \bar{x}_2}}$$

2. t was then calculated by:

$$t = \frac{\bar{X}_1 - \bar{X}_2}{S_{\bar{x}_1 - \bar{x}_2}}$$

FRIEDMAN TEST

NOTE: Test equation is for ranked data with ties between rankings.

$$\chi_r^2 = \frac{n(k-1)\left[\sum_{j=1}^{k}\frac{\left(\sum_{i=1}^{n} X_{ij}\right)^2}{n} - \frac{\left(\sum_{i=1}^{n}\sum_{j=1}^{k} X_{ij}\right)^2}{kn}\right]}{\sum_{i=1}^{n}\sum_{j=1}^{k} X_{ij}^2 - \sum_{i=1}^{n}\frac{\left(\sum_{j=1}^{k} X_{ij}\right)^2}{k}}$$

For Subjective Pilot FOV Pair Ratings:

n = Number of Raters
k = Number of Conditions Being Rated
X_{ij} = Ranked Rating from the i^{th} - Rater for the j^{th} - Condition

For Objective Success/Failure Data:

n = Number of Subjects
k = Number of Parameters Over Which Subject Performance is Being Ranked
X_{ij} = Ranked Performance Level from the i^{th} - Subject for the j^{th} - Parameter

APPENDIX B

SUPPORTIVE DATA RESULTS

SUBJECTIVE DATA RESULTS

SUBJECTIVE DATA RESULTS

F-Test Results on Pilot Rated Workload

SOURCE	DEGREES OF FREEDOM	SUM OF SQUARES	MEAN SQUARE	F VALUE	PROBA-BILITY
PILOT	5	41.81	8.36		
MODE	3	7.59	2.53	0.43	N.S.
PILOT X MODE	15	87.88	5.86		
FOV	2	315.52	157.76	66.62	0.01
PILOT X FOV	10	23.68	2.37		
MODE X FOV	6	10.80	1.80	1.15	N.S.
PILOT X MODE X FOV	30	47.15	1.57		
TASK	2	0.29	0.15	0.65	N.S.
PILOT X TASK	10	22.35	2.24		
MODE X TASK	6	7.54	1.26	1.16	N.S.
PILOT X MODE X TASK	30	32.51	1.08		
FOV X TASK	4	7.86	1.97	6.20	0.01
PILOT X FOV X TASK	20	6.34	0.32		
MODE X FOV X TASK	12	3.33	0.28	0.87	N.S.
PILOT X MODE X FOV X TASK	60	19.08	0.32		

N.S. -- No significance based on 0.05 criterion

SUBJECTIVE DATA RESULTS

T-Test Results on Pilot Rated Workload Between FOV Pairs

Between 6^{o} & 1.5^{o} and 6^{o} & 0.86^{o}	Between 6^{o} & 1.5^{o} and 3^{o} & 0.86^{o}	Between 6^{o} & 0.86^{o} and 3^{o} & 0.86^{o}
$t = 2.99$	$t = 11.15$	$t = 8.16$
$0.025 > p > 0.01$	$p \ll 0.01$	$p \ll 0.01$

SUBJECTIVE DATA RESULTS

Pilot Workload Ratings Ranked Across FOV Pair

FOV Pair / Subject	6° & 1.5°	6° & 0.86°	3° & 0.86°
Pilot 1	1	2	3
Pilot 2	1	2	3
Pilot 3	1	2	3
Pilot 4	1	2	3
Pilot 5	1	2	3
Pilot 6	1	2	3

Friedman Test Results

$\chi_r^2 = 12$

$p = 0.00013$

SUBJECTIVE DATA RESULTS

Pilot Workload Ratings Ranked Between All Combinations of Two FOV Pairs

FOV Pair / Subject	6° & 1.5°	6° & 0.86°		6° & 0.36°	3° & 0.86°		6° & 1.5°	3° & 0.36°
Pilot 1	1	2		1	2		1	2
Pilot 2	1	2		1	2		1	2
Pilot 3	1	2		1	2		1	2
Pilot 4	1	2		1	2		1	2
Pilot 5	1	2		1	2		1	2
Pilot 6	1	2		1	2		1	2

Friedman Test Results

Between Each of the FOV Pairs

$$\chi_r^2 = 6$$

$$p < 0.01$$

SUBJECTIVE DATA RESULTS

Pilot Workload Ratings Ranked Across Task

Task / Subject	Perform Complete Mission	Search for Targets	Fly Designation Turn
Pilot 1	2	3	1
Pilot 2	3	1	2
Pilot 3	1	2	3
Pilot 4	1	2	3
Pilot 5	2	3	1
Pilot 6	2	3	1

Friedman Test Results

$\chi^2_r = 1.00$

$p = 0.74$

SUBJECTIVE DATA RESULTS

Pilot Workload Ratings Ranked Across Rating Parameter

Parameter / Subject	LGB/ CCRP	LG Mav/ LGM	LWLGM/ LGMDT	OVER ALL
Pilot 1	1	2	3	4
Pilot 2	1	2	3	4
Pilot 3	3	1	2	3
Pilot 4	4	3	2	1
Pilot 5	3	1	4	2
Pilot 6	3	2	1	4

Friedman Test Results

$\chi_r^2 = 2.69$

$0.50 > p > 0.30$

SUBJECTIVE DATA RESULTS

F-Test Results on Pilot Rated Effectiveness

SOURCE	DEGREES OF FREEDOM	SUM OF SQUARES	MEAN SQUARE	F VALUE	PROBA-BILITY
PILOT	5	140.02	28.00		
MODE	3	29.30	9.77	1.30	N.S.
PILOT X MODE	15	112.62	7.51		
FOV	2	492.76	246.38	70.52	0.01
PILOT X FOV	10	34.94	3.49		
MODE X FOV	6	8.15	1.36	0.65	N.S.
PILOT X MODE X FOV	30	63.01	2.10		
TASK	3	4.34	1.45	1.03	N.S.
PILOT X TASK	15	20.98	1.40		
MODE X TASK	9	5.48	0.61	0.68	N.S.
PILOT X MODE X TASK	45	40.21	0.89		
FOV X TASK	6	52.30	8.72	5.22	0.01
PILOT X FOV X TASK	30	50.09	1.67		
MODE X FOV X TASK	18	7.82	0.43	0.65	N.S.
PILOT X MODE X FOV X TASK	90	59.74	0.66		

N.S. -- No significance based on 0.05 criterion

SUBJECTIVE DATA RESULTS

T-Test Results on Pilot Rated Effectiveness Between FOV Pairs

Between 6^{o} & 1.5^{o} and 6^{o} & 0.86^{o}	Between 6^{o} & 1.5^{o} and 3^{o} & 0.86^{o}	Between 6^{o} & 0.86^{o} and 3^{o} & 0.86^{o}
$t = 3.37$	$t = 11.56$	$t = 8.19$
$p < 0.01$	$p \ll 0.01$	$p \ll 0.01$

SUBJECTIVE DATA RESULTS

Pilot Effectiveness Ratings Ranked Across FOV Pair

FOV Pair / Subject	6^o & 1.5^o	6^o & 0.86^o	3^o & 0.86^o
Pilot 1	1	2	3
Pilot 2	1	2	3
Pilot 3	1	2	3
Pilot 4	1	2	3
Pilot 5	1	2	3
Pilot 6	1	2	3

Friedman Test Results

$$\chi_r^2 = 12$$

$$p = 0.00013$$

SUBJECTIVE DATA RESULTS

Pilot Effectiveness Ratings Ranked Between All Combinations of Two FOV Pairs

FOV Pair / Subject	6° & 1.5°	6° & 0.86°	6° & 0.86°	3° & 0.86°	6° & 1.5°	3° & 0.86°
Pilot 1	1	2	1	2	1	2
Pilot 2	1	2	1	2	1	2
Pilot 3	1	2	1	2	1	2
Pilot 4	1	2	1	2	1	2
Pilot 5	1	2	1	2	1	2
Pilot 6	1	2	1	2	1	2

Friedman Test Results

Between Each of the FOV Pairs

$$\chi_r^2 = 6$$

$$p < 0.01$$

SUBJECTIVE DATA RESULTS

Pilot Effectiveness Ratings Ranked Across Task

Task / Subject	Perform Complete Mission	Search for Targets	Verify Targets	Fly Designation Turn
Pilot 1	4	3	2	1
Pilot 2	2	1	4	3
Pilot 3	2	3	1	4
Pilot 4	4	2	1	3
Pilot 5	2	3	1	2
Pilot 6	3	2	1	4

Friedman Test Results

$\chi_r^2 = 3.67$

$p = 0.30$

AD-A063 530 GENERAL DYNAMICS CORP FORT WORTH TX FORT WORTH DIV F/G 17/8
F-16 ADVANCED ELECTRO-OPTICAL POD FIELD-OF-VIEW SIMULATION STUD--ETC(U)
DEC 78 F33657-78-C-0290
UNCLASSIFIED FZM-6817 NL

2 OF 2
AD
AD63530

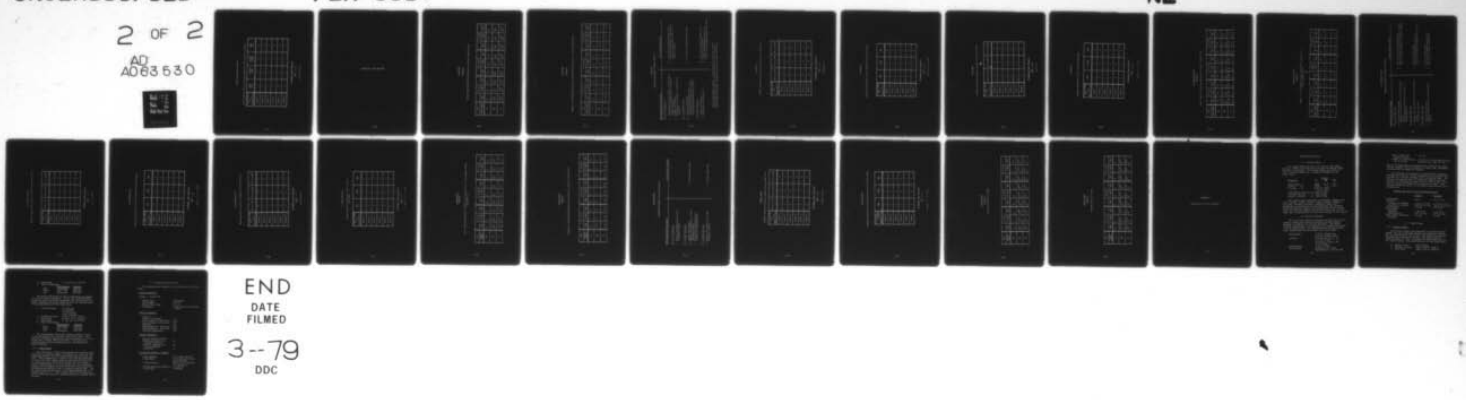

END
DATE
FILMED
3--79
DDC

SUBJECTIVE DATA RESULTS

Pilot Effectiveness Ratings Ranked Across Rating Parameter

Parameter / Subject	LGB/ CCRP	LG Mav/ LGM	LWLGM/ LGMDT	OVER ALL
Pilot 1	1	2	4	3
Pilot 2	4	2	3	1
Pilot 3	1	4	3	2
Pilot 4	1	2	3	4
Pilot 5	2	1	4	3
Pilot 6	4	2	3	1

Friedman Test Results

$\chi^2_r = 0.70$

$0.90 > p > 0.80$

OBJECTIVE DATA RESULTS

LGB/CCRP

RESULTS

Total Time From REO Activation to Target Acquisition

FOV	6^{o} & 1.5^{o}			6^{o} & 0.86^{o}			3^{o} & 0.86^{o}		
REO RANGE	6NM	4.5NM	3NM	6NM	4.5NM	3NM	6NM	4.5NM	3NM
n	15	16	13	16	16	16	14	16	12
$\overline{X}$	9.8 Sec	6.5 Sec	4.8 Sec	13.1 Sec	6.8 Sec	4.7 Sec	9.7 Sec	7.5 Sec	4.3 Sec
S	5.83 Sec	3.78 Sec	1.95 Sec	6.27 Sec	3.43 Sec	2.88 Sec	3.99 Sec	3.54 Sec	2.19 Sec

LGB/CCRP

RESULTS

Number of POD Related Events From REO Activitation to Target Acquisition

FOV	6^{o} & 1.5^{o}			6^{o} & 0.86^{o}			3^{o} & 0.86^{o}		
REO RANGE	6NM	4.5NM	3NM	6NM	4.5NM	3NM	6NM	4.5NM	3NM
n	15	16	13	16	16	16	14	16	12
$\overline{X}$	7.3	7.0	4.8	13.3	7.5	6.4	10.0	8.6	7.7
S	4.60	6.12	1.3	7.74	4.69	4.21	4.37	4.77	4.63

CCRP/LGB

WEAPONS DELIVERY FAILURE ANALYSIS

NON-POD-RELATED FAILURES	POD-RELATED FAILURES
6^{o} & 1.5^{o} FOV Pair	
4 - Late Bomb Releases (Pilot did not have pickle button depressed at computed weapon release) 3 - Target Overflights 1 - No Release (too many G's during toss maneuver)	4 - Pod Line-of-Sight Obscurations 4 - Tracker Break Locks (Pod tracker broke lock and pilot did not re-acquire target)
6^{o} & 0.86^{o} FOV Pair	
2 - Target Overflights 1 - Terrain Obscuration (Pilot inadvertently put mountain or ridge line between aircraft and target)	6 - Pod Line-of-Sight Obscurations
3^{o} & 0.86^{o} FOV Pair	
3 - Target Overflights 1 - No Release (too many G's)	2 - Pod Line-of-Sight Obscurations 3 - Tracker Break Locks 1 - Crash After Target Acquisition (Pilot in head-down display too long)

Target Overflight Failures -- Pilots were briefed that target overflight would result in delivery failure. In instances above pilots could have avoided target overflight but did not.

LGB/CCRP

Target Acquisition Success Ranked Across FOV Pair

FOV Pair / Subject	6° & 1.5°	6° & 0.86°	3° & 0.86°
Pilot 1	2	1	1
Pilot 2	2	3	1
Pilot 3	1	2	2
Pilot 4	1	2	3
Pilot 5	2	1	3
Pilot 6	2	1	3

Friedman Test Results

$\chi_r^2 = 1.29$

$0.74 > p > 0.57$

Target Acquisition Success Ranked Across REO Range

REO RANGE / Subject	6NM	4.5NM	3NM
Pilot 1	1	1	2
Pilot 2	1	2	3
Pilot 3	2	1	1
Pilot 4	1	1	1
Pilot 5	1	1	2
Pilot 6	1	2	2

Friedman Test Results

$X_r^2 = 3.71$

$0.252 > p > 0.184$

LGB/CCRP

Weapons Delivery Success Ranked Across FOV Pair

FOV Pair / Subject	6° & 1.5°	6° & 0.86°	3° & 0.86°
Pilot 1	2	3	1
Pilot 2	1	2	1
Pilot 3	3	1	2
Pilot 4	1	1	2
Pilot 5	2	1	3
Pilot 6	3	1	2

Friedman Test Results

$\chi_r^2 = 1.00$

$p = 0.74$

LGB/CCRP

Weapons Delivery Success Across REO Range

REO RANGE / Subject	6NM	4.5NM	3NM
Pilot 1	1	1	2
Pilot 2	1	1	2
Pilot 3	3	2	1
Pilot 4	1	2	3
Pilot 5	3	2	1
Pilot 6	1	2	3

Friedman Test Results

$\chi_r^2 = 0.57$

$0.956 > p > 0.749$

LG MAVERICK/LGM

RESULTS

Total Time From REO Activation to Target Acquisition

FOV	6^{o} & 1.5^{o}			6^{o} & 0.86^{o}			3^{o} & 0.86^{o}		
REO RANGE	ARI	6NM	4NM	ARI	6NM	4NM	ARI	6NM	4NM
n	15	18	18	16	17	18	14	16	13
$\bar{X}$	36.8 sec	12.3 sec	6.8 sec	39.4 sec	14.0 sec	8.4 sec	43.8 sec	9.3 sec	6.8 sec
S	11.11 sec	6.96 sec	3.36 sec	9.89 sec	6.92 sec	4.83 sec	19.02 sec	5.05 sec	4.56 sec

LG MAVERICK/LGM

RESULTS

Number of Pod Related Events from REO Activation to Target Acquisition

FOV	6^o & 1.5^o			6^o & 0.86^o			3^o & 0.86^o		
REO RANGE	ART	6NM	4NM	ART	6NM	4NM	ART	6NM	4NM
n	15	18	18	16	17	18	14	16	13
$\bar{X}$	22.3	13	7.8	23.7	14.7	8.7	25.1	10.1	9.5
S	11.22	7.72	3.22	12.66	5.68	4.83	11.58	4.37	6.01

LG MAVERICK/LGM

WEAPONS DELIVERY FAILURE ANALYSIS

NON-POD-RELATED FAILURES	POD-RELATED FAILURES
6^{o} & 1.5^{o} FOV Pair	
3 - Terrain Obscurations	1 - Pod Line-of-Sight Obscuration
7 - Missile Deliveries Out of Off Boresight Limits	5 - Tracker Break Locks (pod tracker broke lock and pilot did not reacquire target)
1 - Switchology Problem (Pilot forgot to uncage missile)	
6^{o} & 0.86^{o} FOV Pair	
3 - Missile Deliveries Out of Off Boresight Limits	4 - Tracker Break Locks
1 - Terrain Obscuration	1 - Crash After Target Acquisition (pilot in head-down display too long)
3^{o} & 0.86^{o} FOV Pair	
1 - Terrain Obscuration	2 - Tracker Break Locks
1 - Missile Delivery Out of Off Boresight Limits	1 - Pod Line-of-Sight Obscuration
	1 - Crash After Target Acquisition

LG MAVERICK/LGM

Target Acquisition Success Ranked Across FOV Pair

FOV Pair / Subject	6° & 1.5°	6° & 0.86°	3° & 0.86°
Pilot 1	2	1	3
Pilot 2	1	1	2
Pilot 3	2	1	3
Pilot 4	1	2	1
Pilot 5	1	2	3
Pilot 6	1	2	2

Friedman Test Results

$\chi_r^2 = 5.17$

$0.142 > p > 0.072$

LG MAVERICK/LGM

Target Acquisition Success Ranked Across REO Range

REO RANGE / Subject	ARI	6NM	4NM
Pilot 1	2	1	2
Pilot 2	2	1	2
Pilot 3	2	1	1
Pilot 4	2	1	1
Pilot 5	2	3	1
Pilot 6	2	1	3

Friedman Test Results

$X_r^2 = 3.25$

$0.252 > p > 0.184$

LG MAVERICK/LGM

Weapons Delivery Success Ranked Across FOV Pair

FOV Pair / Subject	6° & 1.5°	6° & 0.86°	3° & 0.86°
Pilot 1	2	1	2
Pilot 2	3	1	2
Pilot 3	1	1	2
Pilot 4	2	3	1
Pilot 5	3	2	1
Pilot 6	2	3	1

Friedman Test Results

$\chi_r^2 = 1.71$

$0.57 > p > 0.43$

LG MAVERICK/LGM

Wespons Delivery Success Ranked Across
REO Range

REO RANGE / Subject	ARI	6NM	4NM
Pilot 1	1	1	2
Pilot 2	1	2	2
Pilot 3	2	1	2
Pilot 4	1	2	1
Pilot 5	1	2	1
Pilot 6	2	1	3

Friedman Test Results

$\chi^2_r = 1.75$

$0.570 \geq p > 0.430$

LWLGM/LGMDT
RESULTS

Total Time from Head-Up Target Area Acquisition to Head-Down Target Acquisition

FOV	6^o & 1.5^o			6^o & 0.86^o			3^o & 0.86^o		
POP-UP RANGE	7NM	5.5NM	4NM	7NM	5.5NM	4NM	7NM	5.5NM	4NM
n	11	5	8	10	13	7	13	8	10
$\bar{X}$	12.4 sec	11.8 sec	8.2 sec	13.6 sec	9.0 sec	8.3 sec	16.3 sec	10.5 sec	9.6 sec
S	4.81 sec	1.85 sec	4.32 sec	7.95 sec	4.49 sec	5.25 sec	5.72 sec	4.7 sec	4.39 sec

LWLGM/LGMDT

RESULTS

Number of Pod Related Events from Pop-Up to Target Acquisition

FOV	6^{o} & 1.5^{o}			6^{o} & 0.86^{o}			3^{o} & 0.86^{o}		
POP-UP RANGE	7NM	5.5NM	4NM	7NM	5.5NM	4NM	7NM	5.5NM	4NM
n	11	5	8	10	13	7	13	8	10
$\overline{X}$	15.5	15	12	15	13	12.5	18	15	12
S	6.71	5.26	5.19	7.23	6.20	8.62	8.21	7.21	4.64

LWLGM/LGMDT

WEAPONS DELIVERY FAILURE ANALYSIS

NON-POD-RELATED FAILURES	POD-RELATED FAILURES
6^{o} & 1.5^{o} FOV Pair	
1 - Missile Delivered Out of Off Boresight Limits	
6^{o} & 0.86^{o} FOV Pair	
2 - Target Overflights 1 - Missile Delivered Out of Off Boresight Limits 1 - Switchology Proglem (pilot forgot to uncage missile)	4 - Tracker Break Locks
3^{o} & 0.86^{o} FOV Pair	
1 - Missile Delivered Out of Off Boresight Limits	1 - Tracker Break Lock

LWLGM/LGMDT

Wespons Delivery Success Ranked Across FOV Pair

FOV Pair / Subject	6° & 1.5°	6° & 0.86°	3° & 0.86°
Pilot 1	2	2	1
Pilot 2	3	2	1
Pilot 3	2	3	1
Pilot 4	1	2	2
Pilot 5	1	2	2
Pilot 6	2	3	1

Friedman Test Results

$\chi_r^2 = 4.67$

$0.142 > p > 0.072$

LWLGM/LGMDT

Weapons Delivery Success Ranked Across Pop-Up Range

POP-UP RANGE / Subject	7NM	5.5NM	4NM
Pilot 1	2	1	1
Pilot 2	1	2	2
Pilot 3	1	3	2
Pilot 4	1	2	3
Pilot 5	1	2	3
Pilot 6	1	3	2

Friedman Test Results

$\chi_r^2 = 5.14$

$0.142 > p > 0.072$

LWLGM/LGMDT

RESULTS

Target Acquisition Range

FOV	6^{o} & 1.5^{o}			6^{o} & 0.86^{o}			3^{o} & 0.86^{o}		
POP-UP RANGE	7NM	5.5NM	4NM	7NM	5.5NM	4NM	7NM	5.5NM	4NM
n	11	5	8	10	13	7	13	8	10
$\bar{X}$	23247 ft	9776 ft	7890 ft	21108 ft	14398 ft	10046 ft	18181 ft	14367 ft	9830 ft
S	7534 ft	3546 ft	3197 ft	7648 ft	5174 ft	5355 ft	5611 ft	4366 ft	4723 ft

LWLGM/LGMDT

RESULTS

Weapon Delivery Range

FOV	6^{o} & 1.5^{o}			6^{o} & 0.86^{o}			3^{o} & 0.86^{o}		
POP-UP RANGE	7NM	5.5NM	4NM	7NM	5.5NM	4NM	7NM	5.5NM	4NM
n	11	5	7	8	12	6	13	8	9
$\bar{X}$	16729 ft	8656 ft	7430 ft	15688 ft	13304 ft	9708 ft	15063 ft	11330 ft	9438 ft
S	3652 ft	3631 ft	2833 ft	3292 ft	4066 ft	4732 ft	3685 ft	3900 ft	4386 ft

APPENDIX C

Simulation Facility Details

SIMULATION FACILITY

1.1 Terrain Board

The terrain model was 80' x 40' with a fiber glass surface. Three foot high mirrors ringed the terrain model for terrain extension. The terrain model was scaled to 1200:1 for the simulation. Simulation parameters for 1200:1 were:

Parameter		1200:1 FT	NM	KM
Slant Range	to	96000	15.8	29.3
Lateral	to	48000	7.9	14.6
Altitude	to	12000 Ft (Max)		
		84 Ft (Min)		
Longitudinal Velocity	to	12000 Ft/Sec		
Vertical Velocity	to	7200 Ft/Sec		
Lateral Velocity	to	4800 Ft/Sec		

The terrain model consisted of mountains, plains, harbors, streams, ridges, forests, dams, tunnels, highways, railroads, bridges, airports, buildings, docks, etc. Topography was rolling hills modelled after West Germany. Choice of materials used in the manufacture of the terrain model was based on weather and sun resistance and, at the same time, a presentation of realistic targets to the sensors.

1.2 Motion Simulation

The 3-D terrain model was mounted on 30 trucks, and 10 central trucks with compound bearings provided lateral guidance in addition to vertical guidance. The trucks allowed translation of the assembly in a longitudinal direction on three tracks. The characteristics of the terrain model longitudinal drive assembly are listed below.

Displacement	$\pm$ 80 ft (probes up) $\pm$ 78 ft (probes down)
Velocity	Accuracy at min $\pm$ 1.0% at 0.01 ft/sec Accuracy at max $\pm$ .05% at 10 ft/sec
Acceleration	$\pm$ 10.0 ft/sec^2
Positioning	Accuracy $\pm$ 0.1 inch Repeatability .02 inch max

Small signal frequency response	3.0 cps
Weight of longitudinal drive system	24,000 lbs. static and rolling friction less than 250 lbs.

The 3-D terrain model was mechanized to simulate the longitudinal movement of the aircraft in flight; and, therefore, accounted for one degree of freedom.

The remaining two degrees of translational freedom to simulate vertical and lateral movement of the aircraft were provided by a lateral carriage and a horizontal beam. The lateral carriage was free to translate laterally and was attached to a horizontal beam which was free to move in the vertical direction between two supporting columns. The operating characteristics of the lateral and vertical drive systems were:

Lateral and Vertical Drive Characteristics

	Lateral	Vertical
Displacement	38 ft	25 ft 7 in.
Velocity		
Accuracy at minimum	$\pm$ 1.0% at 0.004	$\pm$ 1.0% at 0.00
Accuracy at maximum	.05% at 4.0 ft/s	.05% at 6.0 ft/s
Acceleration	4 ft/s^2	6.0 ft/s^2
Positioning		
Accuracy	$\pm$ .02 inch	$\pm$ .02 inch
Repeatability	.005 in. max	.005 in. max
Small Signal Frequency Response	3.0 cps	3.0 cps

1.3 Video System

1.3.1 Optical Probes

Two optical probes were employed to provide wide FOV imagery for the windscreen display and narrow FOV imagery for the simulation of the EO pod. The wide FOV probe was a Schemimpflug corrected probe which had essentially an infinite depth of field, allowing low level operation over the terrain board. The specifications of this probe were:

1. Field of View — 50° circular
2. Minimum altitude — 63mm ≈ 250 ft (1200:1)
3. Near focus — 25mm ≈ 100 ft (1200:1)

4. Resolution 2.3 arc min at 25% MTV
5. Servo Performance

	Displacement	Velocity
Roll	Continuous	360°/sec
Pitch	+25°, -90°	100°/sec
Yaw	Continuous	360°/sec

The narrow FOV probe was used to generate the imagery for the EO probe simulation. It was also a Schemimpflug corrected probe which had essentially an infinite depth of field, allowing low level operation over the terrain board. The specifications of this probe were:

1. Fields-of-View 6° circular
   4° circular
   1.5° circular
   0.86° circular
2. Minimum altitude 12 mm ≈ 50 ft (1200:1)
3. Near focus 30 mm ≈ 120 ft (1200:1)
4. Resolution 17 arc sec at 25% MTV
5. Servo Performance

	Displacement	Velocity
Roll	Continuous	360°/sec
Pitch	+25°, -90°	100°/sec
Yaw	Continuous	360°/sec

The longitudinal separation between entrance pupils of the two probes was 12 inches (1200 scale feet). The altitude separation between the entrance pupils of the two probes was 2 inches (200 scale feet). The resulting parallex effects were compensated with software on the hybrid computer.

1.3.2 Video System

Two 1200 lines, 60 MHz high resolution TV systems were used with the optical probes to generate the video for the windscreen display and the radar/electro-optical (REO) display. Both systems had a variable line rate and bandwidth so that a 512 line signal could be generated for the study. In conjunction with the optical probes, the TV systems yielded resolutions of 4.4 arc minutes for the windscreen probe at the 50-degree field-of-view and 17 arc seconds for the REO display probe at the 1.5-degree field-of-view. The TV systems had the capability to be underscanned down to a maximum ratio of 2:1. The 3-degree field-of-view employed in the study was created by underscanning the 4-degree field-of-view.

1.4 Analog/Digital Facility

The computational elements of the facility are listed below.

Digital Computer

Sigma 5 - Triple CPU

Memory Size	160K words
Word Length	32 bits
Memory Cycle Time	1.0 μs
Arithmetic	Fixed point and floating point

Analog Computers

231R-V's	
Number of Consoles	6
Total number of amplifiers	1496
Quarter-square multipliers	276
Resolvers	30
Potentiometers - Servo Set	900
Potentiometers - Hand Set	140
Function generators	120

Hybrid Interface

Digital Computer/231R-V	
Multiplying Digital to Analog Converters	56
Analog to Digital Converter Channels	48
12 BIT DAC	64

Peripheral Devices - Sigma 5

2 Card Readers	400 & 1500 car/min
4 Mag Tapes	75 inches per second 800 bits/inch
2 Line Printers	800 & 1000 lines/min 132 char/line
2 Fixed Head Disk Memories	6.0 Mbytes
1 Disk Pack	48 Mbytes